CRACKING OF COATED MATERIALS UNDER

TRANSIENT THERMAL STRESSES

A.A. Rizk and F. Erdogan

June 1988

Lehigh University, Bethlehem, PA 18015

CRACKING OF COATED MATERIALS UNDER

TRANSIENT THERMAL STRESSES

A.A. Rizk and F. Erdogan

June 1988

Lehigh University, Bethlehem, PA   18015

CRACKING OF COATED MATERIALS UNDER
TRANSIENT THERMAL STRESSES[*]

by

A.A. Rizk and F. Erdogan
Lehigh University, Bethlehem, PA 18015

ABSTRACT

In this paper the crack problem for a relatively thin layer bonded to a very thick substrate under "thermal shock" conditions is considered. The effect of surface cooling rate is studied by assuming the temperature boundary condition to be a ramp function. Among the crack geometries considered are the edge crack in the coating layer, the broken layer, the edge crack going through the interface, the undercoat crack in the substrate and the embedded crack crossing the interface. The primary calculated quantity is the stress intensity factor at various singular points and the main variables are the relative sizes and locations of cracks, the time, and the duration of the cooling ramp. The problem is solved and rather extensive results are given for two material pairs, namely a stainless steel layer welded on a ferritic medium and a ceramic coating on a steel substrate.

1. Introduction

A common failure mode in many structural components that consist of a relatively thin coating and a substrate is the cracking of the coating, the substrate, or both under transient thermal stresses. Cladded pressure vessels under thermal shock, and certain microelectronic devices and ceramic-coated metal parts under rapidly changing thermal environments may be mentioned as some typical examples for such components. Very often in transient thermal stress analysis it is assumed that the relevant thermal boundary condition is a step change in temperature. In the fracture analysis even though this assumption would lead to conservative bounds for the stress intensity factors, in most cases it is not a realistic representation of the actual boundary conditions.

The broad aim of this study is to provide the solution needed for assessing the crack propagation and arrest process in a coated medium

-1-

CRACKING OF COATED MATERIALS UNDER
TRANSIENT THERMAL STRESSES[*]

by

A.A. Rizk and F. Erdogan
Lehigh University, Bethlehem, PA 18015

ABSTRACT

In this paper the crack problem for a relatively thin layer bonded
to a very thick substrate under "thermal shock" conditions is considered.
The effect of surface cooling rate is studied by assuming the temperature
boundary condition to be a ramp function. Among the crack geometries
considered are the edge crack in the coating layer, the broken layer, the
edge crack going through the interface, the undercoat crack in the sub-
strate and the embedded crack crossing the interface. The primary calcu-
lated quantity is the stress intensity factor at various singular points
and the main variables are the relative sizes and locations of cracks,
the time, and the duration of the cooling ramp. The problem is solved
and rather extensive results are given for two material pairs, namely
a stainless steel layer welded on a ferritic medium and a ceramic coat-
ing on a steel substrate.

1. Introduction

A common failure mode in many structural components that consist of
a relatively thin coating and a substrate is the cracking of the coating,
the substrate, or both under transient thermal stresses. Cladded pres-
sure vessels under thermal shock, and certain microelectronic devices and
ceramic-coated metal parts under rapidly changing thermal environments
may be mentioned as some typical examples for such components. Very
often in transient thermal stress analysis it is assumed that the rele-
vant thermal boundary condition is a step change in temperature. In the
fracture analysis even though this assumption would lead to conservative
bounds for the stress intensity factors, in most cases it is not a real-
istic representation of the actual boundary conditions.

The broad aim of this study is to provide the solution needed for
assessing the crack propagation and arrest process in a coated medium

---

containing a certain initial flaw and subjected to transient thermal loading. In a simplified fracture analysis this requires the determination of the stress intensity factors as functions of time and dimensions concerning the size and location of the crack. In order to study the influence of the thermal boundary conditions on the fracture process, in this study the rise time of the surface temperature is assumed to be an additional variable in formulating the crack problem.

The crack problem is solved under the following simplifying assumptions: (i) the medium consists of two dissimilar linear isotropic homogeneous materials bonded along an ideal plane interface; (ii) the crack lies in xz plane, the constraints in z direction are such that the problem may be treated as either a plane strain or a generalized plane stress problem in xy plane, and the thermal boundary conditions are independent of y; (iii) the thickness of the substrate is very large compared to that of the coating, hence for small times the main features of the problem may be recovered by approximating the medium by a layer bonded to an elastic half space; (iv) all thermoelastic coupling effects and the temperature dependence of thermoelastic coefficients are negligible; and (v) the transient thermal stress problem is quasistatic, that is the inertia effects are negligible. The previous studies on dynamic thermoelasticity seem to bear out the validity of the last assumption (see, for example [1] and [2]).

The thermal shock problem for hollow cylinders containing an axial or a circumferential crack was considered in [3]-[5], where it was assumed that the thermal boundary condition is a step function in temperature. In [3] the axisymmetric circumferential crack problem was analyzed for a homogeneous hollow cylinder. The same problem was studied in [4] by assuming that the cylinder is homogeneous in elastic but non-homogeneous in thermal properties, simulating the cladded pressure vessels. In [5] the crack is assumed to be axial, that is, in the rz plane and the coating is approximated by a "membrane" in the elasticity solution and is assumed to be a homogeneous continuum in solving the diffusion problem.

2. Temperature Distribution

Consider the nonhomogeneous thermoelastic medium shown in Fig. la. Assume that initially the medium is at a constant temperature T_∞ and starting at t=0 the temperature of the surface x=0 is (suddenly or gradually) changed to T_0 and is held constant at T_0 for $t > t_0$ (Fig. lb). Defining

$$T_i(x,t) - T_\infty = \theta_i(x,t) \, , \quad i=1,2 \, , \tag{1}$$

the differential equations and the boundary conditions for the heat conduction problem may be expressed as[*]

$$\frac{\partial^2 \theta_i}{\partial x^2} = \frac{1}{D_i} \frac{\partial \theta_i}{\partial t} \, , \quad (i=1,2) \, , \tag{2}$$

$$\theta_i(x,0) = 0, \quad (i=1,2) \, , \tag{3}$$

$$\theta_1(h,t) = \theta_2(h,t), \quad k_1{}' \, \frac{\partial \theta_1(h,t)}{\partial x} = k_2{}' \, \frac{\partial \theta_2(h,t)}{\partial x} \, , \tag{4}$$

$$\theta_2(\infty,t) = 0 \, , \tag{5}$$

$$\theta_1(0,t) = \theta_0 H(t) \, , \quad \theta_0 = T_0 - T_\infty \, , \quad \text{or} \tag{6}$$

$$\theta_1(0,t) = \frac{\theta_0}{t_0} \, [tH(t) - (t-t_0)H(t-t_0)] \, , \quad \theta_0 = T_0 - T_\infty \, . \tag{6a}$$

The solution of (2) subject to (3)-(6) may be obtained in a straightforward manner by using Laplace transforms (see, for example, [6],[7]). Defining the dimensionless quantities

$$x' = x/h, \quad \beta = \sqrt{D_1/D_2} \, , \quad \eta = \beta k_1{}'/k_2{}' \, , \quad \tau = tD_1/h^2 \, , \tag{7}$$

for the boundary condition (6) the temperature distributions in the two materials are found to be

$$\frac{\theta_1(x',\tau)}{\theta_0} = 1 - \frac{2\eta}{\pi} \int_0^\infty \frac{e^{-\tau s^2} \sin x' s}{s(\cos^2 s + \eta^2 \sin^2 s)} \, ds \, , \quad 0 < x' < 1 \, , \tag{8}$$

[*] See the List of Symbols for notation

$$\frac{\theta_2(x',\tau)}{\theta_0} = 1 - \frac{2}{\pi} \int_0^\infty \{e^{-\tau s^2}[\cos s \sin\beta(x'-1)s$$

$$+ \eta\sin s \cos\beta(x'-1)s]/[s(\cos^2 s + \eta^2\sin^2 s)]\}ds, \quad 1<x'<\infty \ . \quad (9)$$

Similarly, if the temperature boundary condition at x=0 is given by the ramp function shown by (6a), we obtain

$$\frac{\theta_1(x',\tau)}{\theta_0} = \frac{\tau}{\tau_0} - \frac{2\eta}{\pi\tau_0} \int_0^\infty \frac{(1-e^{-\tau s^2})\sin x's \ ds}{s^3(\cos^2 s + \eta^2\sin^2 s)} \ , \quad 0<x'<1, \ 0<\tau<\tau_0 \ , \quad (10)$$

$$\frac{\theta_1(x',\tau)}{\theta_0} = 1 - \frac{2\eta}{\pi\tau_0} \int_0^\infty \frac{e^{-\tau s^2}(e^{-\tau_0 s^2}-1)\sin x's}{s^3(\cos^2 s + \eta^2\sin^2 s)} \ ds, \quad 0<x'<1, \ \tau>\tau_0 \quad (11)$$

$$\frac{\theta_2(x',\tau)}{\theta_0} = \frac{\tau}{\tau_0} - \frac{2}{\pi\tau_0} \int_0^\infty \{(1-e^{-\tau s^2})[\cos s \sin\beta(x'-1)s$$

$$+ \eta\sin s \cos\beta(x'-1)]/[s^3(\cos^2 s + \eta^2\sin^2 s)]\}ds, \quad x'>1, \ 0<\tau<\tau_0,$$
$$(12)$$

$$\frac{\theta_2(x',\tau)}{\theta_0} = 1 - \frac{2}{\pi\tau_0} \int_0^\infty \{e^{-\tau s^2}(e^{\tau_0 s^2}-1)[\cos s \sin\beta(x'-1)s$$

$$+ \eta\sin s \cos\beta(x'-1)s]/[s^3(\cos^2 s + \eta^2\sin^2 s)]\}ds, \quad x'>1, \ \tau>\tau_0$$
$$(13)$$

where
$$\tau_0 = t_0 D_1/h^2 \ . \quad (14)$$

3. Thermal Stresses in the Uncracked Medium

In the uncracked medium subjected to thermal initial and boundary conditions (3)-(6) x and t are the only independent variables, the medium is unconstrained in x direction and is fully constrained in y and z

directions. For the thermal stresses we thus have

$$\sigma^T_{ixx} = 0, \; \epsilon_{ixy} = \epsilon_{ixz} = \epsilon_{iyz} = \epsilon_{iyy} = \epsilon_{izz} = 0, \; \sigma^T_{iyy} = \sigma^T_{izz}, \; (i=1,2). \quad (15)$$

From (15) it follows that

$$\sigma^T_{1yy}(x,t) = \sigma^T_{1zz}(x,t) = - \frac{E_1 \alpha_1 \theta_1(x,t)}{1-\nu_1} , \; 0<x<h, \; t>0 , \quad (16)$$

$$\sigma^T_{2yy}(x,t) = \sigma^T_{2zz}(x,t) = - \frac{E_2 \alpha_2 \theta_2(x,t)}{1-\nu_2} , \; x>h, \; t>0 . \quad (17)$$

By defining

$$\sigma_0 = - \frac{E_1 \alpha_1 \theta_0}{1-\nu_1} , \; x' = \frac{x}{h} , \; \tau = \frac{tD_1}{h^2} , \quad (18)$$

the stresses may also be expressed in the following normalized form:

$$\frac{\sigma^T_{1yy}(x',\tau)}{\sigma_0} = \frac{\theta_1(x',\tau)}{\theta_0} , \; 0<x'<1 , \; \tau>0 , \quad (19)$$

$$\frac{\sigma^T_{2yy}(x',\tau)}{\sigma_0} = \frac{E_2 \alpha_2 (1-\nu_1)}{E_1 \alpha_1 (1-\nu_2)} \frac{\theta_2(x',\tau)}{\theta_0} , \; x'>1, \; \tau>0 . \quad (20)$$

4. The Crack Problem

Consider now the crack problem shown in Fig. 1a. Since the problem is linear, one may consider the solutions due to thermal and mechanical loads separately. One may also simplify the problem by considering the stress state in the medium as the sum of two solutions. The first is obtained by solving the problem for the uncracked medium under the pre-scribed thermal and mechanical loads, and the second is found from the cracked medium in which the equal and opposite of the stresses given by the first solution acting on the crack surfaces are the only external loads. In this paper the primary interest is in the stress intensity

factors due to transient thermal stresses. It is, therefore, sufficient to consider the problem under the crack surface tractions given by (19) and (20) (with the opposite signs).

The plane elasticity problem shown in Fig. 1 requires the solution of the following equilibrium equations

$$(\kappa_i - 1)\nabla^2 u_i + 2(\frac{\partial^2 u_i}{\partial x^2} + \frac{\partial^2 v_i}{\partial x \partial y}) = 0 \ , \ (i=1,2) \ , \tag{21}$$

$$(\kappa_i - 1)\nabla^2 v_i + 2(\frac{\partial^2 u_i}{\partial x \partial y} + \frac{\partial^2 v_i}{\partial y^2}) = 0 \ , \ (i=1,2) \ , \tag{22}$$

subject to

$$\sigma_{1xx}(0,y) = 0 \ , \ \sigma_{1xy}(0,y) = 0 \ , \ 0 < y < \infty \ , \tag{23}$$

$$\sigma_{1xx}(h,y) = \sigma_{2xx}(h,y) \ , \ \sigma_{1xy}(h,y) = \sigma_{2xy}(h,y) \ , \ 0 < y < \infty \ , \tag{24}$$

$$u_{1x}(h,y) = u_2(h,y) \ , \ v_1(h,y) = v_2(h,y) \ , \ 0 < y < \infty \ , \tag{25}$$

$$\sigma_{1ij}(x,y) \to 0 \ , \ \sigma_{2ij}(x,y) \to 0 \ , \ (x^2+y^2) \to \infty \ , \ (i,j=x,y) \ , \tag{26}$$

$$\sigma_{1xy}(x,0) = 0, \ 0 < x < h; \ \sigma_{2xy}(x,0) = 0, \ h < x < \infty \ , \tag{27}$$

$$\sigma_{1yy}(x,0) = p_1(x) = -\sigma_{1yy}^T(x,t) \ , \ a_1 < x < b_1 \ , \tag{28a}$$

$$v_1(x,0) = 0, \ 0 < x < a_1, \ b_1 < x < h \ , \tag{28b}$$

$$\sigma_{2yy}(x,0) = p_2(x) = -\sigma_{2yy}^T(x,t) \ , \ a_2 < x < b_2 \ , \tag{29a}$$

$$v_2(x,0) = 0, \ h < x < a_2 \ , \ b_2 < x < \infty, \tag{29b}$$

where, in the usual notation u_k and v_k, (k=1,2) are the x and y-components of the displacement vector and σ_{1ij} and σ_{2ij}, (i,j=x,y) are the stresses in materials 1 and 2, respectively. Note that y=0 is a plane of symmetry and, hence, the problem is considered for y>0 only. The stresses and displacements are related through

$$\sigma_{ixx} = \frac{\mu_i}{\kappa_i - 1} \left[(\kappa_i + 1) \frac{\partial u_i}{\partial x} + (3 - \kappa_i) \frac{\partial v_i}{\partial y} \right] , \quad (i=1,2) , \tag{30}$$

$$\sigma_{iyy} = \frac{\mu_i}{\kappa_i - 1} \left[(3 - \kappa_i) \frac{\partial u_i}{\partial x} + (\kappa_i + 1) \frac{\partial v_i}{\partial y} \right] , \quad (i=1,2) , \tag{31}$$

$$\sigma_{ixy} = \mu_i \left(\frac{\partial u_i}{\partial y} + \frac{\partial v_i}{\partial x} \right) , \quad (i=1,2) . \tag{32}$$

The differential equations (21) and (22) are solved by expressing u_i and v_i, (i=1,2) in terms of Fourier integrals [7],[8]. Thus, by defining

$$\phi_1(x) = \frac{\partial}{\partial x} v_1(x, +0) , \quad \phi_2(x) = \frac{\partial}{\partial x} v_2(x, +0) , \tag{33}$$

and by following the procedure described, for example, in [8], the problem may be reduced to the following system of integral equations (see [7] for details):

$$\int_{a_1}^{b_1} \left[\frac{1}{s-x} + k_{11}(x,s) \right] \phi_1(s) ds + \int_{a_2}^{b_2} k_{12}(x,s) \phi_2(s) ds$$

$$= \frac{\pi(1+\kappa_1)}{4\mu_1} p_1(x) , \quad a_1 < x < b_1 , \tag{34}$$

$$\int_{a_1}^{b_1} k_{21}(x,s) \phi_1(s) ds + \int_{a_2}^{b_2} \left[\frac{1}{s-x} + k_{22}(x,s) \right] \phi_2(s) ds$$

$$= \frac{\pi(1+\kappa_2)}{4\mu_2} p_2(x) , \quad a_2 < x < b_2 , \tag{35}$$

subject to

$$\int_{a_1}^{b_1} \phi_1(x) dx = 0 , \quad \int_{a_2}^{b_2} \phi_2(x) dx = 0 \tag{36a,b}$$

if $0<a_1<b_1<a_2<b_2<\infty$. The kernels k_{ij}, $(i,j=1,2)$ are of the form

$$k_{ij}(x,s) = \int_0^\infty G_{ij}(x,s,\alpha)d\alpha \ , \ (i,j=1,2) \tag{37}$$

where the functions G_{ij} are given in Appendix A.

To improve the accuracy in evaluating the integrals shown in (37) and, most importantly, to examine the singular behavior of the solution for cracks intersecting the interface or the boundary, (37) is rewritten as

$$k_{ij}(x,s) = \int_0^\infty [G_{ij}(x,s,\alpha)-G_{ij}^\infty(x,s,\alpha)]d\alpha + \int_0^\infty G_{ij}^\infty(x,s,\alpha)d\alpha,$$

$$(i,j=1,2) \ , \tag{38}$$

where G_{ij}^∞ is the asymptotic form of G_{ij} for large values of α. In this problem, after some lengthy but relatively straightforward analysis, it may be shown that (see [8] and also [7] for details)

$$k_{ij}(x,s) = k_{ij}^f(x,s) + k_{ij}^s(x,s) \ , \ (i,j=1,2) \ , \tag{39}$$

$$k_{ij}^f(x,s) = \int_0^\infty [G_{ij}(x,s,\alpha)-G_{ij}^\infty(x,s,\alpha)]d\alpha \ , \ (i,j=1,2) \ , \tag{40}$$

$$k_{ij}^s(x,s) = \int_0^\infty G_{ij}^\infty(x,s,\alpha)d\alpha \ , \ (i,j=1,2) \ , \tag{41}$$

where the functions k_{ij}^f are bounded in the closed intervals $[a_1,b_1]$ and $[a_2,b_2]$, including $a_1=0$, $b_1=h$, $a_2=h$ and the (singular) kernels k_{ij}^s are found to be

$$k_{11}^s = k_{11}^{s1} + k_{11}^{s2} \tag{42}$$

$$k_{11}^{s1} = -\frac{1}{s+x} + \frac{6x}{(s+x)^2} - \frac{4x^2}{(s+x)^3} \ , \ (a_1<(s,x)<b_1) \ , \tag{43}$$

$$k_{11}^{s2} = \frac{c_{11}}{(2h-x-s)} + \frac{c_{12}(h-x)}{(2h-x-s)^2} + \frac{c_{13}(h-x)^2}{(2h-x-s)^3} \ , \quad (a_1 <(x,s)< b_1) \ , \qquad (44)$$

$$c_{11} = \frac{3(m-1)}{2(m+\kappa_1)} - \frac{m\kappa_2-\kappa_1}{2(m\kappa_2+1)} \ , \quad c_{12} = -6\,\frac{m-1}{m+\kappa_1} \ , \quad c_{13} = 4\,\frac{m-1}{m+\kappa_1} \ ,$$

$$m = \frac{\mu_1}{\mu_2} \ , \qquad (45)$$

$$k_{12}^{s} = \frac{d_{11}}{s-x} + \frac{d_{12}(x-h)}{(s-x)^2} \ , \quad (a_1<x<b_1, \ a_2<s<b_2) \ , \qquad (46)$$

$$d_{11} = \frac{3(\kappa_1+1)}{2(m+\kappa_1)} - \frac{\kappa_1+1}{2(m\kappa_2+1)} \ , \quad d_{12} = \frac{\kappa_1+1}{m+\kappa_1} - \frac{\kappa_1+1}{m\kappa_2+1} \ , \qquad (47)$$

$$k_{21}^{s} = \frac{d_{21}}{x-s} + \frac{d_{22}(x-h)}{(x-s)^2} \ , \quad (a_1<s<b_1, \ a_2<x<b_2), \qquad (48)$$

$$d_{21} = -\,\frac{3m(\kappa_2+1)}{2(m\kappa_2+1)} + \frac{m(\kappa_2+1)}{2(m+\kappa_1)} \ , \quad d_{22} = \frac{m(\kappa_2+1)}{m\kappa_2+1} - \frac{m(\kappa_2+1)}{m+\kappa_1} \ , \qquad (49)$$

$$k_{22}^{s} = \frac{c_{21}}{(s+x-2h)} + \frac{c_{22}(x-h)}{(s+x-2h)^2} + \frac{c_{23}(x-h)^2}{(s+x-2h)^3} \ , \quad (a_2<(x,s)<b_2 \ , \qquad (50)$$

$$c_{21} = -\,\frac{m\kappa_2-\kappa_1}{2(m+\kappa_1)} + \frac{3(m-1)}{2(m\kappa_2+1)} \ , \quad c_{22} = -6\,\frac{m-1}{m\kappa_2+1} \ , \quad c_{23} = 4\,\frac{m-1}{m\kappa_2+1} \ . \qquad (51)$$

We now observe that as long as the crack tips are away from the free surface and the interface (i.e., for $a_1>0$, $b_1<h$ and $a_2>h$), the kernels k_{ij}^{s} are bounded and may be treated, along with k_{ij}^{f}, as Fredholm kernels. In this case the integral equations (34) and (35) have only an ordinary Cauchy singularity and may be solved by using any one of the standard techniques [9]. One may also note that in the limiting cases of an edge crack ($a_1=0$), a crack terminating at the interface ($b_1=h$ or $a_2=h$), or the crack crossing the interface ($a_2=h=b_2$), if the variables x and s approach the end points 0 or h together, then the kernels $k_{ij}^{s}(x,s)$ become unbounded and, consequently, would also contribute to the singular behavior of the solution. Such kernels are defined as generalized Cauchy kernels [9].

5. Singularities of the Solution

To examine the singular behavior of the solution of integral equations (34) and (35) we observe that (a) the left hand sides of (34) and (35) represent the stress components $\sigma_{1yy}(x,0)$ and $\sigma_{2yy}(x,0)$ outside as well as inside the cracks in materials 1 and 2, respectively, and (b) the known functions p_1 and p_2, defined inside the cracks, are bounded but $\sigma_{iyy}(x,0)$, $(i=1,2)$ may be discontinuous and unbounded as x approaches the crack tips from outside. With these observations the singular nature of ϕ_1 and ϕ_2 and the stress state around the crack tips may be determined by a systematic application of the function theoretic method to (34) and (35). To do this we define the following sectionally holomorphic functions of the complex variable $z=x+iy$

$$F_j(z) = \frac{1}{\pi} \int_{a_j}^{b_j} \frac{\phi_j(s)}{s-z} ds , \quad (j=1,2) , \tag{52}$$

and express the unknown functions ϕ_j, $(j=1,2)$ as [10]

$$\phi_j(s) = \frac{g_j(s)}{(s-a_j)^{\gamma_j}(b_j-s)^{\beta_j}} , \quad (a_j<s<b_j) ,$$

$$0<\mathrm{Re}(\gamma_j,\beta_j)<1, \quad (j=1,2) , \tag{53}$$

where the unknown functions $g_j(s)$ are Hölder-continuous in the closed intervals $a_j \le s \le b_j$, $(j=1,2)$ and are nonzero at the end points. Following the asymptotic analysis given in [10], the leading terms in (52) may be separated and F_j may be expressed as follows:

$$F_j(z) = \frac{g_j(a_j)e^{\pi i \gamma_j}}{(b_j-a_j)^{\beta_j}\sin\pi\gamma_j} \frac{1}{(z-a_j)^{\gamma_j}} - \frac{g_s(b_j)}{(b_j-a_j)^{\gamma_j}\sin\pi\beta_j} \frac{1}{(z-b_j)^{\beta_j}} + G_j(z),$$

$$(j=1,2), \tag{54}$$

where the functions $G_j(z)$ are bounded everywhere except possibly at the

respective end points near which they may have a weaker singularity of the form

$$|G_j(z)| < \frac{A_{jk}}{|z-c_{jk}|^{\varepsilon_{jk}}} \ , \ (j=1,2) \ , \qquad ,$$

$$c_{j1} = a_j \ , \ \varepsilon_{j1} < \mathrm{Re}(\gamma_j) \ , \ c_{j2} = b_j \ , \ \varepsilon_{j2} < \mathrm{Re}(\beta_j) \ . \qquad (55)$$

In (55) k=1 and k=2 correspond to end points a_j and b_j, and A_{jk} and ε_{jk} are positive constants.

From the Plemelj formula

$$\frac{1}{\pi} \int_{a_j}^{b_j} \frac{\phi_j(s)}{s-x} \, ds = \frac{1}{2} [F_j^+(x)+F_j^-(x)] \ , \ (j=1,2) \qquad (56)$$

and (54) it may be shown that

$$\frac{1}{\pi} \int_{a_j}^{b_j} \frac{\phi_j(s)}{s-x} \, ds = \frac{g_j(a_j)\cot\pi\gamma_j}{(b_j-a_j)^{\beta_j}(x-a_j)^{\gamma_j}} - \frac{g_j(b_j)\cot\pi\beta_j}{(b_j-a_j)^{\gamma_j}(b_j-x)^{\beta_j}} + G_j(x) \ ,$$

$$a_j < x < b_j \ , \ (j=1,2) \ . \qquad (57)$$

In integral equations (34) and (35) there are also other "Cauchy-type" integrals coming from the generalized Cauchy kernels $k_{ij}^S(x,s)$. From (43)-(50) and (52) it may be seen that all these integrals can be expressed in terms of a Cauchy integral of the form

$$\frac{1}{\pi} \int_{a_j}^{b_j} \frac{\phi_j(s)}{s-z_0} \, ds = F_j(z_0) \ , \ (j=1,2) \qquad (58)$$

where z_0 is outside the corresponding branch cut and hence $F_j(z)$ is holomorphic at $z=z_0$ (e.g., $z_0=-x<(a_1,0)$ in k_{11}^{S1}, $z_0=2h-x>(b_1,h)$ in k_{11}^{S2}, $z_0=2h-x<(a_2,h)$ in k_{22}^S, $z_0=x<h<s$ in k_{12}^S and $z_0=x>h>s$ in k_{21}^S). From (58) we also observe that

$$\frac{1}{\pi}\int_{a_j}^{b_j}\frac{\phi_j(s)}{(s-z_0)^2}\,ds=\frac{d}{dz_0}F_j(z_0)\ ,\ \frac{1}{\pi}\int_{a_j}^{b_j}\frac{\phi_j(s)}{(s-z_0)^3}\,ds=\frac{1}{2}\frac{d^2}{dz_0^2}F_j(z_0).$$

(59)

Since the remaining kernels k_{ij}^f are all bounded in their respective closed intervals, with the density functions as defined by (53) the corresponding integrals would also be bounded for all values of x. Thus, in the asymptotic analysis they may be combined with the other bounded terms p_1 and p_2.

The singular behavior of ϕ_1 and ϕ_2 may now be determined for any location of the crack tips (i.e., for $a_1\geq0$, $b_1\leq h$, $a_2\geq h$) by substituting from (53)-(59) into (34) and (35), and multiplying both sides of the equations by $(x-a_j)^{\gamma_j}$, or $(b_j-x)^{\beta_j}$, and letting $x\to a_j$, $x\to b_j$ for $a_1>0$, $b_1<h$, $a_2>h$, and by x^{γ_1}, $(h-x)^{\beta_1}$, $(x-h)^{\gamma_2}$ and letting $x\to0$, $x\to h-0$, $x=h+0$ for the limiting crack tip locations $a_1=0$, $b_1=h$, $a_2=h$. In the standard case of cracks embedded into homogeneous materials, that is for $a_1>0$, $b_1<h$, $a_2>h$, k_{ij}^s as well as k_{ij}^f are bounded and the only contribution to the singularity comes from the Cauchy kernels $(s-x)^{-1}$ in (34) and (35). Thus, since $g_j(a_j)\neq0$, $g_j(b_j)\neq0$, from (57), (55), (53), (34) and (35) it may easily be seen that

$$\cot\pi\gamma_j=0,\ \cot\pi\beta_j=0;\ \gamma_j=1/2,\ \beta_j=1/2\ ,$$

(60)

leading to the standard results for the embedded cracks, namely

$$\phi_j(x)=\frac{g_j(x)}{\sqrt{(x-a_j)(b_j-x)}}\ ,\ (a_j<x<b_j)\ ,\ (j=1,2)\ .$$

(61)

The characteristic equations for γ_j and β_j corresponding to various other special crack geometries may be obtained by using the asymptotic expressions given in this section and the related generalized Cauchy kernels $k_{ij}^s(x,s)$. If, for example $a_1=0$ (i.e., the case of an edge crack), then following the procedure outlined above, substituting from (43), (54), (57) (with $a_1=0$) and (59) into (34), multiplying both sides by

x^{γ_1}, letting $x \to 0$, and by observing that $g_1(0) \neq 0$, the characteristic equation for γ_1 is obtained to be

$$\cos\pi\gamma_1 - 2(\gamma_1-1)^2 + 1 = 0 . \tag{62}$$

The only acceptable root of (62) is $\gamma_1=0$, that is, as expected at $x=0$ the derivative of the crack surface displacement is found to be bounded. If $b_1<h$, $a_2>h$, then the results found for β_1, γ_2 and β_2 in (60) would, of course, remain valid.

Consider now the case of a crack tip terminating at the interface. Let, for example, $b_1=h$, $a_1 \geq 0$, $a_2>h$. Clearly for the embedded crack (a_2,b_2) (35) would again give $\gamma_2=\beta_2=-1/2$. Also, regardless of the location of the crack tip $x=b_1$, (34) would give $\gamma_1=-1/2$ for $a_1>0$ and $\gamma_1=0$ for $a_1=0$. Thus, to determine β_1 (defined in (53) for $b_1=h$) it is sufficient to consider only the singular kernels $(s-x)^{-1}$ and $k_{11}^{s2}(x,s)$ in (34). By substituting from (57)-(59) (with $b_1=h$, $z_0=2h-x$) into (34) and by separating the terms that are singular at $x=b_1=h$, it may be shown that

$$- \frac{g_1(h)\cot\pi\beta_1}{(h-a_1)^{\gamma_1}} \frac{1}{(h-x)^{\beta_1}} + \frac{g_1(h)}{(h-a_1)^{\gamma_1}\sin\pi\beta_1} [c_{11} + c_{12}(h-x)\frac{d}{dx}$$

$$+ \frac{1}{2} c_{13}(h-x)^2 \frac{d^2}{dx^2}] \frac{1}{(h-x)^{\beta_1}} = H(x) , \quad a_1<x<h , \tag{63}$$

where $H(x)$ represents all other terms in (34) that are bounded at $x=h$. After carrying out the differentiation, if we multiply both sides in (63) by $(h-x)^{\beta_1}$, let $x \to h$ and observe that $g_1(h) \neq 0$, we find

$$\cos\pi\beta_1 - \frac{1}{2} c_{13}\beta_1(\beta_1+1) - c_{12}\beta_1 - c_{11} = 0 , \tag{64}$$

where the coefficients c_{1j} are given by (45).

Similarly, for relative crack tip locations $0 \leq a_1<b_1<h = a_2<b_2$ we find

$$\cos\pi\gamma_2 + \frac{1}{2} c_{23}\gamma_2(\gamma_2+1) + c_{22}\gamma_2 + c_{21} = 0 \qquad (65)$$

with c_{2j} as given by (51).

Finally, to examine the singular behavior of ϕ_1 and ϕ_2 at $x=h$ for a crack crossing the interface we let $0\leq a_1<b_1=h=a_2<b_2$ and observe that the end point $x=h$ is common to both cracks. In (53) we must, therefore, have

$$\beta_1 = \gamma_2 = \beta, \quad 0<Re(\beta)<1, \quad (b_1=h=a_2) . \qquad (66)$$

In this case by separating the terms that are bounded at the common end point $x=h$ the integral equations (34) and (35) may be expressed as

$$\frac{1}{\pi}\int_{a_1}^{h} [\frac{1}{t-x} + k_{11}^{s2}(x,s)]\phi_1(s)ds + \frac{1}{\pi}\int_{h}^{b_2} k_{12}^{s}(x,s)\phi_2(s)ds = H_1(x) ,$$
$$a_1<x<h , \qquad (67)$$

$$\frac{1}{\pi}\int_{a_1}^{h} k_{21}^{s}(x,s)\phi_1(s)ds + \frac{1}{\pi}\int_{h}^{b_2} [\frac{1}{s-x} + k_{22}^{s}(x,s)]\phi_2(s)ds = H_2(x) ,$$
$$h<x<b_2 , \qquad (68)$$

where H_1 and H_2 represent all other terms in (34) and (35) bounded at $x=h$. By substituting now from (57) with $b_1=h$, $a_2=h$, $\beta_1=\gamma_2=\beta$, and (54), (58) and (59) with $z_0=2h-x$ and $z_0=x$ into (67) and (68) we obtain

$$\frac{-g_1(h)\cot\pi\beta}{(h-a_1)^{\gamma_1}(h-x)^{\beta}} + \frac{g_1(h)}{(h-a_1)^{\gamma_1}\sin\pi\beta} [c_{11}+c_{12}(h-x)\frac{d}{dx} + \frac{c_{13}}{2}(h-x)^2\frac{d^2}{dx^2}]\frac{1}{(h-x)^{\beta}}$$

$$+ \frac{g_2(h)}{(b_2-h)^{\beta_2}\sin\pi\beta} [d_{12}(x-h)\frac{d}{dx} + d_{11}]\frac{1}{(h-x)^{\beta}} = H_1(x), \quad a_1<x<h, \quad (69)$$

$$\frac{-g_1(h)}{(h-a_1)^{\gamma_1}\sin\pi\beta} [d_{22}(x-h)\frac{d}{dx} - d_{21}] \frac{1}{(x-h)^{\beta}} + \frac{g_2(h)\cot\pi\beta}{(b_2-h)^{\beta_2}} \frac{1}{(x-h)^{\beta}}$$

$$+ \frac{g_2(h)}{(b_2-h)^{\beta_2}\sin\pi\beta} [c_{21}-c_{22}(x-h)\frac{d}{dx} + \frac{c_{23}}{2}(x-h)^2\frac{d^2}{dx^2}]\frac{1}{(x-h)^{\beta}} = H_2(x), \quad h<x<b_2.$$
$$(70)$$

Multiplying (69) and (70) respectively by $(h-x)^\beta$ and $(x-h)^\beta$ and letting $x \to h$, it may be shown that

$$[c_{11}+c_{12}\beta+\tfrac{1}{2}c_{13}(1+\beta)\beta-\cos\pi\beta] \frac{g_1(h)}{(h-a_1)^{\gamma_1}\sin\pi\beta}$$

$$+ (d_{11}-d_{12}\beta) \frac{g_2(h)}{(b_2-h)^{\beta_2}\sin\pi\beta} = 0$$

$$(d_{21}+d_{22}\beta) \frac{g_1(h)}{(h-a_1)^{\gamma_1}\sin\pi\beta}$$

$$+ [\cos\pi\beta+c_{21}+\beta c_{22}+\tfrac{1}{2}\beta(\beta+1)c_{23}] \frac{g_2(h)}{(b_2-h)^{\beta_2}\sin\pi\beta} = 0 \quad . \quad (71a,b)$$

Since $g_1(h)$ and $g_2(h)$ are nonzero, from (71) we obtain the following characteristic equation to determine β and the relationship between $g_1(h)$ and $g_2(h)$:

$$[c_{11}+c_{12}\beta+\frac{c_{13}}{2}\beta(1+\beta)-\cos\pi\beta][c_{21}+c_{22}\beta+\frac{c_{23}}{2}\beta(1+\beta)+\cos\pi\beta]$$

$$-(d_{11}-d_{12}\beta)(d_{21}+d_{22}\beta) = 0 \quad , \quad 0<Re(\beta)<1 \quad , \qquad (72)$$

$$\frac{g_1(h)}{g_2(h)} = -\frac{(h-a_1)^{\gamma_1}}{(b_2-h)^{\beta_2}} \frac{c_{21}+c_{22}\beta+\tfrac{1}{2}c_{23}\beta(1+\beta)+\cos\pi\beta}{d_{21}+d_{22}\beta} \quad . \qquad (73)$$

A close examination of the characteristic equations (64), (65) and (72) would show that in each case the acceptable leading root is real for all material combinations.

It may be remarked that for $a_1>0$ the solution of the integral equations (34) and (35) contain two arbitrary constants [10], [9]. In the case of two non-intersecting embedded cracks (that may include $b_1=h$ or

a_2=h) the single-valuedness conditions (36) are used to determine these constants. For a_1=0, $b_1 \neq a_2$, only (35) contains an arbitrary constant which is determined from (36b). For the crack crossing the interface (36) reduce to the following single condition which accounts for only one of the constants:

$$\int_{a_1}^{h} \phi_1(x)dx + \int_{h}^{b_2} \phi_2(x)dx = 0 . \tag{74}$$

The additional condition needed to determine the second constant is provided by (73).

6. Stress Intensity Factors

Recalling that the left hand sides of equations (34) and (35) represent $\sigma_{1yy}(x,0)$ and $\sigma_{2yy}(x,0)$ outside as well as inside the cracks, from (34) and (35) we can write

$$\frac{1+\kappa_i}{4\mu_i} \sigma_{iyy}(x,0) = \frac{1}{\pi} \int_{a_j}^{b_j} [\frac{\delta_{ij}}{s-x} + k_{ij}^s(x,s)]\phi_j(s)ds + M_i(x), \quad (i=1,2)$$

$$\tag{75a,b}$$

where functions M_1 and M_2 correspond to the terms that are bounded at the end points. If the cracks are embedded into the respective homogeneous materials (i.e., if $0<a_1<b_1<h<a_2<b_2$), then the kernels k_{ij}^s are bounded for all values of x and s making also only bounded contributions to $\sigma_{iyy}(x,0)$. In this case we observe that for x outside the cracks the Cauchy integrals in (75) may be expressed by (58) and (54), which, upon separating the singular terms, and substituting into (74) give

$$\sigma_{kyy}(x,0) = \frac{4\mu_k}{1+\kappa_k} [\frac{g_k(a_k)i}{\sqrt{b_k-a_k} \sqrt{x-a_k}} - \frac{g_k(b_k)}{\sqrt{b_k-a_k} \sqrt{x-b_k}} + P_k(x)], \quad (k=1,2) \tag{76}$$

where P_1 and P_2 represent all the bounded terms on the left hand side of (34) and (35). Defining now the mode I stress intensity factors by

$$k_1(a_j) = \lim_{x \to a_j - 0} \sqrt{2(a_j - x)} \; \sigma_{jyy}(x,0), \quad (j=1,2) \tag{77}$$

$$k_1(b_j) = \lim_{x \to b_j + 0} \sqrt{2(x - b_j)} \; \sigma_{jyy}(x,0) \;, \; (j=1,2) \tag{78}$$

from (75) it is seen that

$$k_1(a_j) = \frac{4\mu_j}{1+\kappa_j} \frac{g_j(a_j)}{\sqrt{(b_j - a_j)/2}} \;, \; k_1(b_j) = -\frac{4\mu_j}{1+\kappa_j} \frac{g_j(b_j)}{\sqrt{(b_j - a_j)/2}} \;. \tag{79}$$

We now consider the crack terminating at the interface and let $0 \le a_1$, $b_1 = h$, $h < a_2 < b_2$. Again, let the stress intensity factor at $x=h$ be defined in terms of the local cleavage stress, which in this case is $\sigma_{2yy}(x,0)$, $x > h$. Thus, analogous to (78) we may define

$$k_1(h) = \lim_{x \to h+0} \sqrt{2} \; (x-h)^{\beta_1} \sigma_{2hh}(x,0) \;. \tag{80}$$

On the other hand, keeping only the terms that may contribute to the stress singularity and by substituting from (48), (75b) may be expressed as

$$\frac{1+\kappa_2}{4\mu_2} \sigma_{2yy}(x,0) = \frac{1}{\pi} \int_{a_1}^{h} \left(\frac{-d_{21}}{s-x} + \frac{d_{22}(x-h)}{(s-x)^2} \right) \phi_1(s)ds + Q_1(x) \;, \tag{81}$$

where $Q_1(x)$ represent all the remaining terms that are bounded at $x=h$. Since x is outside the cut (a_1, h), (58), (59) and (54) may be used in (81) with $z_0 = x$, giving

$$\frac{1+\kappa_2}{4\mu_2} \sigma_{2yy}(x,0) = -d_{21}F_1(x) + d_{22}(x-h) \frac{d}{dx} F_1(x) + Q_1(x) \tag{82}$$

or

$$\sigma_{2yy}(x,0) = \frac{4\mu_2}{1+\kappa_2} \frac{g_1(h)}{(h-a_1)^{\gamma_1} \sin\pi\beta_1} (d_{21}+d_{22}\beta_1) \frac{1}{(x-h)^{\beta_1}} + Q_2(x) \tag{83}$$

where Q_2 again is bounded or, at most may have a singularity weaker[*] than $(x-h)^{-\beta_1}$. From (83) it is seen that the cleavage stress σ_{2yy} has a singularity at $x=h$ with power β_1 and from (80) and (83) it follows that

$$k_1(h) = \frac{4\mu_2}{1+\kappa_2} \frac{\sqrt{2}\, g_1(h)}{(h-a_1)^{\gamma_1}\sin\pi\beta_1}(d_{21}+d_{22}\beta_1) \tag{84}$$

where β_1 is the acceptable leading root of (64), g_1 is defined by (53), d_{21} and d_{22} are given by (49), and $\gamma_1=1/2$ for $a_1>0$ and $\gamma_1=0$ for $a_1=0$.

Similarly, for the crack in material 2 and terminating at the interface, i.e., for $0\leq a_1<b_1<h$, $h=a_2<b_2$, from the asymptotic examination of $\sigma_{1yy}(x,0)$, $x<h$ we find

$$k_1(h) = \lim_{x\to h-0} \sqrt{2}\,(h-x)^{\gamma_2}\sigma_{1yy}(x,0)$$

$$= \frac{4\mu_1}{1+\kappa_1} \frac{\sqrt{2}\, g_2(h)}{(b_2-h)^{\beta_2}\sin\pi\gamma_2}(d_{11}-d_{12}\gamma_2) \tag{85}$$

where γ_2 is given by (65), d_{11} and d_{12} by (47) and $\beta_2=1/2$.

In the case of a crack crossing the interface the stresses as well as the displacement derivatives would have a singularity at $x=h$ of the form $r^{-\beta}$, r being the radial distance from the point $x=h$, $y=0$ and β the root of (72). In this problem of particular interest are the normal and shear cleavage stresses σ_{xx} and σ_{xy} along the bond line $x=h$. The expressions for $\sigma_{xx}(h,y)$ and $\sigma_{xy}(h,y)$ may be obtained in terms of ϕ_1 and ϕ_2 by going back to the main formulation of the problem[**].

---

[*] This is due to the possible singular terms coming from $G_1(z)$ that appear in (54) and has the behavior as given by (55), and from the fact that the characteristic equation (64) may have more than one root satisfying $0<\mathrm{Re}(\beta_1)<1$.

[**] Note that, because of continuity we have $\sigma_{1xx}(h,y)=\sigma_{2xx}(h,y)=\sigma_{xx}(h,y)$ and $\sigma_{1xy}(h,y)=\sigma_{2xy}(h,y)=\sigma_{xy}(h,y)$.

After somewhat lengthy analysis and upon separating the singular parts
of the kernels it can be shown that (see [7] for details)

$$\sigma_{xx}(h,y) = \frac{2\mu_2}{1+\kappa_2} \sum_1^2 \frac{1}{\pi} \int_{a_j}^{k_j} [k_{3j}^s(y,s) + k_{3j}^f(y,s)]\phi_j(s)ds, \quad (0<y) , \qquad (86)$$

$$\sigma_{xy}(h,y) = \frac{2\mu_2}{1+\kappa_2} \sum_1^2 \frac{1}{\pi} \int_{a_j}^{b_j} [k_{4j}^s(y,s) + k_{4j}^f(y,s)]\phi_j(s)ds, \quad (0<y) , \qquad (87)$$

where $b_1=a_2=h$, the kernels k_{ij}^f, ($i=3,4$; $j=1,2$) are of the Fredholm type
and the generalized Cauchy kernels k_{ij}^s, ($i=3,4$; $j=1,2$) are given in Appen-
dix B. In (86) and (87) only k_{ij}^s contribute to the stress singularity
at ($y=0$, $x=h$). The singular terms in (86) and (87) may be evaluated by
using again (58), (59) and (54). For example, by substituting from

$$\phi_1(s) = \frac{g_1(s)}{(s-a_1)^{\gamma_1}(h-s)^\beta} , \quad (a_1<s<h) \qquad (88)$$

into (86), using the equations (B1), (54) and (58), the first term in
(86) may be obtained as

$$\frac{1}{\pi} \int_{a_1}^h \frac{\phi_1(s)ds}{(h-s)^2+y^2} = \frac{1}{2}\frac{1}{\pi} \int_{a_1}^h (\frac{1}{h-s+iy} + \frac{1}{h-s-iy})\phi_1(s)ds$$

$$= \frac{g_1(h)}{2(h-a_1)^{\gamma_1}\sin\frac{\pi\beta}{2}}\frac{1}{y^\beta} + R(y) \qquad (89)$$

where R represents the terms that are bounded at ($y=0$, $x=h$). It is then
clear that the leading terms in the asymptotic expressions for $\sigma_{xx}(h,y)$
and $\sigma_{xy}(h,y)$ will be of the form $y^{-\beta}$, where β is the root of (72). We
may now define the following stress intensity factors to characterize the

stress singularity at $(y=0, x=h)$:

$$k_{xx} = \lim_{y \to +0} y^\beta \sigma_{xx}(h,y), \quad k_{xy} = \lim_{y \to +0} y^\beta \sigma_{xy}(h,y) \quad . \tag{90a,b}$$

By using the results of the form (89), from (86), (87) and (88) it may then be shown that

$$k_{xx} = - \frac{\mu_2}{(1+\kappa_2)\sin\frac{\pi\beta}{2}} \left[\frac{A+(1-2\beta)B}{(h-a_1)^{\gamma_1}} g_1(h) - \frac{B+(1-2\beta)A}{(b_2-a)^{\beta_2}} g_2(h) \right] , \tag{91}$$

$$k_{xy} = \frac{\mu_2}{(1+\kappa_2)\cos\frac{\pi\beta}{2}} \left[\frac{A-(1-2\beta)B}{(h-a_1)^{\gamma_1}} g_1(h) + \frac{B-(1-2\beta)A}{(b_2-h)^{\beta_2}} g_2(h) \right] \tag{92}$$

$$A = \frac{m(1+\kappa_2)}{m\kappa_2+1} , \quad B = \frac{m(\kappa_2+1)}{m+\kappa_1} , \quad m = \mu_1/\mu_2 , \tag{93}$$

where $\beta_2=1/2$, $\gamma_1=1/2$ for $a_1>0$ and $\gamma_1=0$ for $a_1=0$.

Two stress intensity factors defined by (90) at the same point is simply for convenience. As one might expect and as seen from (73), (91) and (92), $g_1(h)$ and $g_2(h)$ are not independent and there is only one parameter characterizing the stress singularity. If (r,θ) are the polar coordinates with the origin at the point $(x=h, y=0)$, for small values of r the stresses may be expressed as

$$\sigma_{ij}(r,\theta) \cong \frac{k_o}{r^\beta} f_{ij}(\theta) , \quad (i,j=x,y) , \quad 0\le\theta\le\pi \tag{94}$$

Thus, from (90) and (94) it follows that

$$k_{xx} = k_o f_{xx}(\pi/2) , \quad k_{xy} = k_o f_{xy}(\pi/2) \quad . \tag{95}$$

7. On the Solution of the Integral Equations

For numerical solution the integral equations (34) and (35) are first normalized to read

$$\frac{1}{\pi} \int_{-1}^{1} [\frac{\delta_{ij}}{\rho-r} + m_{ij}(r,\rho)]\psi_j(\rho)d\rho = \frac{1+\kappa_i}{4\mu_i} q_i(r) , \quad -1<r<1, \quad (i=1,2) \qquad (96)$$

where

$$r = \frac{2}{b_i-a_i} (x - \frac{b_i+a_i}{2}), \quad \rho = \frac{2}{b_i-a_i} (s - \frac{b_i+a_i}{2}) , \quad q_i(r) = p_i(x),$$

$$m_{ij}(r,\rho) = \frac{b_j-a_j}{2} k_{ij}(x,s), \quad \psi_j(\rho)=\phi_j(s) = \frac{f_j(\rho)}{(1+\rho)^{\gamma_j}(1-\rho)^{\beta_j}}. \qquad (97)$$

The unknown functions f_1 and f_2 are real and bounded and may be determined by using any one of the techniques available for solving singular integral equations [9]. In this paper it is assumed that

$$f_j(\rho) = \sum_{0}^{N_j} A_{jn}\rho^n , \quad -1<\rho<1 , \quad (j=1,2) . \qquad (98)$$

The unknown coefficients are then determined by using the special formulas and the procedure developed in [11] and [12] for various crack configurestions.

8. Results and Discussion

As examples for the thermal shock problem described in the previous sections we consider two material combinations. Material pair A corresponds to a stainless steel layer welded on a much thicker ferritic steel medium approximating cladded pressure vessels of very large diameters. Material pair B represents a ceramic layer (Material 1) bonded to a thick steel substrate (Material 2). The properties of the two material combinations are given in Table 1. Since the problem is formulated in terms of dimensionless quantities, it is sufficient to consider only the ratios shown in the table.

Table 1. Properties of material pairs used in examples

	k_2/k_1	D_2/D_1	α_2/α_1	E_2/E_1	ν_2/ν_1
Material pair A	3	3	0.75	1	1
Material pair B	3.385	4.070	2.2939	0.6111	1

Figures 2 and 3 show some sample results for the normalized stresses σ^T_{iyy}/σ_0 defined by (19) and (20) in the material pair A. Note that these are essentially the plots of normalized temperatures (see equations (16)-(20)). Comparison of the two figures clearly shows the influence of ramp cooling on the transient thermal stresses, particularly for small values of time[(*)]. Stress intensity factors for various crack geometries in the material pair A are shown in Figures 4-16 (see Fig. 1 for notation). In Figures 4-16 all stress intensity factors are normalized with respect to

$$k_0 = \sigma_0 \sqrt{\ell} \ , \quad \sigma_0 = - \frac{E_1 \alpha_1 \theta_0}{1-\nu_1} \ , \tag{99}$$

where ℓ is the total crack length for an edge crack (i.e., $\ell=b_1$ for $a_1=0$, $b_1<h$, and $\ell=b_2$ for $a_1=0$, $b_1=h=a_2$) and the half crack length for an internal crack. The parameter τ_0 defined by

$$\tau_0 = t_0 D_1 / h^2 \tag{100}$$

is the measure of the rate of change of surface temperature during thermal shock, t_0 being the actual duration of the ramp (see (6a) and Fig. 1b).

Figure 4 shows the variation of the normalized stress intensity factor $k_1(b_1)/\sigma_0\sqrt{b_1}$ for an edge crack and for $\tau_0=0$ with the Fourier

---

(*) In the materials used for a clad thickness h=6 mm. $t \doteq 10\tau$, t and τ being the real and normalized times (in units of seconds) (see (18)).

number $\tau=tD_1/h^2$ representing the normalized time. Note that in the material pair A $E_1=E_2$ and $\nu_1=\nu_2$. Consequently as $\tau\to\infty$ k_1/k_0 would approach the uniformly loaded half plane solution of 1.1215 (see, for example [11]). This asymptotic trend may be seen in Fig. 4. For a fixed crack length $b_1=0.5h$ the influence of the cooling rate on the surface $x=0$ as measured by τ_0 is shown in Fig. 5. It is seen that for small values of time this influence could be quite considerable.

The stress intensity factor given in Fig. 4 as well as that given in all subsequent figures are presented in normalized form and the normalizing stress intensity, k_0 always contains a length parameter (as, for example, in $k_0=\sigma_0\sqrt{b_1}$ for the case shown in Fig. 4, b_1 being the crack length). Thus, in considering questions relating to fracture propagation and fracture instability, the normalized stress intensities must be multiplied by k_0 before they are compared with the fracture toughness, K_{IC} or used in a subcritical crack growth model. One consequence of this in connection with the example described in Fig. 4 is that $k_1(b_1)$ is a monotonously increasing function of both crack length and time implying an unstable fracture process.

For an edge crack crossing the interface the results similar to Figures 4 and 5 are shown in Figures 6 and 7. For each crack length the figures also show the asymptotic values of the stress intensity factor as $\tau\to\infty$. The stress intensity factors $k_1(a_2)$ and $k_1(b_2)$ for an under-clad crack are shown in Figures 8-11. Again, the figures also show the asymptotic values of k_1 as $\tau\to\infty$. One may note that in material pair A, despite the large differences in thermal coefficients α, D and k', the elastic constants E and ν for the two materials are the same. Consequently, for a crack terminating at the interface we have $\gamma_2=1/2$ (Figures 8-11), $\beta_1=1/2$ (Fig. 12) and for a crack crossing the interface $\beta=0$ (Figures 6,7,13-16). Figure 12 shows the stress intensity factor for an edge crack terminating at the interface ($b_1=h$). Figures 13-16 show the results for material pair A containing an internal crack crossing the interface ($0<a_1<b_1=h=a_2<b_2<\infty$). Figures 13 and 14 show the influence of ramp duration τ_0 on the stress intensity factors for a fixed crack geometry, $a_1=0.2h$, $b_2=2h$. Figures 15 and 16 gives the stress

intensity factors for an under-clad crack growing into the clad. The figures also show the asymptotic values of the stress intensity factors for $t \rightarrow \infty$.

The results for the material pair B are given in Figures 17-25. Figures 17 and 18 show some sample results for the transient thermal stresses $\sigma_{1yy}^T(x,t)$ and $\sigma_{2yy}^T(x,t)$ obtained for $\tau_0=0$ and $\tau_0=60$. Again, from (16) and (17) it follows that these are essentially the temperature distributions in the composite medium. For these materials the stress discontinuity at the interface is given by (see (19) and (20))

$$\frac{\sigma_{2yy}^T(h,t)}{\sigma_{1yy}^T(h,t)} = \frac{E_2\alpha_2(1-\nu_1)}{E_1\alpha_1(1-\nu_2)} = 1.4019 \tag{101}$$

Figures 19 and 20 show the normalized stress intensity factor for an edge crack in material 1. The limiting case for the edge crack terminating at the interface is shown in Fig. 21. In this case for the material combination under consideration (64) gives the power of singularity as $\beta_1=0.552538$. The normalizing stress intensity factor used in Fig. 21 is defined by

$$k_0 = \sigma_1 h^{\beta_1} \tag{102}$$

The results for an edge crack going through the interface (i.e., $a_1=0$, $b_1=h=a_2<b_2<\infty$, Fig. 1) are shown in Figures 22-25. Figure 22 shows the effect of the ramp duration τ_0 on the crack tip stress intensity factor $k_1(b_2)$ for a fixed crack length $b_2=2h$. The influence of the crack length b_2 on $k_1(b_2)$ is shown in Fig. 23. Finally, Figures 24 and 25 show the stress intensity factors k_{xx} and k_{xy} governing tensile and shear cleavage stresses at interface, $(x=h, y>0)$.

References

1. E. Sternberg and J.G. Chakravorty, "On inertia effects in a transient thermoelastic problem", J. Appl. Mech., Vol. 26, Trans. ASME, pp. 503-508, 1959.

2. E. Sternberg and J.G. Chakravorty, "Thermal shock in an elastic body with a spherical cavity", Q. Appl. Math., Vol. 17, pp. 205-220, 1959.

3. H.F. Nied and F. Erdogan, "The transient thermal stress problem for a circumferentially cracked hollow cylinder", J. Thermal Stresses, Vol. 6, pp. 1-14, 1983.

4. H.F. Nied, "Thermal shock in a circumferentially cracked hollow cylinder with cladding", J. Engineering Fracture Mechanics, Vol. 20, pp. 113-137, 1984.

5. Renji Tang and F. Erdogan, "Transient thermal stresses in a reinforced hollow disk or cylinder containing a radial crack", J. of Engineering for Gas Turbines and Power, Trans. ASME, Vol. 107, pp. 212-219, 1985.

6. H.S. Carslaw and J.C. Jaeger, Conduction of Heat in Solids, Oxford University Press, 1950.

7. A.A. Rizk, "Cracking of a layered medium on an elastic foundation under thermal shock", Ph.D. Dissertation, Lehigh University, 1988.

8. F. Erdogan and V. Biricikoglu, "Two bonded half planes with a crack going through the interface", Int. J. Engng. Sci., Vol. 11, pp. 745-766, 1973.

9. F. Erdogan, "Mixed boundary value problems in Mechanics", Mechanics Today, S. Nemat-Nasser, ed., Vol. 4, pp. 1-86, 1978.

10. N.I. Muskhelishvili, Singular Integral Equations, P. Noordhoff N.V., 1953.

11. A.C. Kaya and F. Erdogan, "On the solution of integral equations with strongly singular kernels", Quarterly of Applied Mathematics, Vol. XLV, pp. 105-122, 1987.

12. A.C. Kaya and F. Erdogan, "On the solution of integral equations with a generalized Cauchy kernel", Quarterly of Applied Mathematics, Vol. XLV, pp. 455-469, 1987.

APPENDIX A

The functions $G_{ij}(x,s,\alpha)$ appearing in equation (37)

$$G_{11} = [-H_1 - (\frac{\kappa_2+3}{2} + \alpha x)\frac{H_3}{D}]e^{\alpha x} + [H_5 - (\frac{\kappa_1+3}{2} - \alpha x)\frac{H_7}{D}]e^{-\alpha x} \ ,$$

$$G_{12} = \frac{\kappa_1+1}{\kappa_2+1} \{[-H_2 - (\frac{\kappa_1+3}{2} + \alpha x)\frac{H_4}{D}]e^{\alpha x} + [H_6 - (\frac{\kappa_2+3}{2} - \alpha x)\frac{H_8}{D}]e^{-\alpha x}\} \ ,$$

$$G_{21} = \frac{\kappa_2+1}{\kappa_1+1} [H_9 - (\frac{\kappa_2+3}{2} - \alpha x)H_{11}]e^{-\alpha x} \ ,$$

$$G_{22} = [H_{10} - (\frac{\kappa_2-3}{2} - \alpha x)H_{12}]e^{-\alpha x} \ ; \qquad\qquad (A1-A4)$$

$$H_1 = \frac{1}{2}[(1-2\alpha t)e^{-\alpha t} + (H_7 - \kappa_1 H_3)\frac{1}{D}] \ ,$$

$$H_2 = \frac{1}{2D} (H_8 - \kappa_1 H_4) \ ,$$

$$H_3 = d_2 d_3[1+2\alpha h(2\alpha t-1)]e^{-\alpha(t+2h)} - d_1 d_3 e^{-\alpha(t+4h)}$$
$$\qquad -d_2 d_3[1+2\alpha(t-h)]e^{\alpha(t-2h)} + d_1 d_3(1+2\alpha t)e^{\alpha(t-4h)} \ ,$$

$$H_4 = d_2 d_5 e^{-\alpha t} - \{d_1 d_5 + 2d_3 d_5 \alpha h[1-2\alpha(t-h)]\}e^{-\alpha(t+2h)} \ ,$$

$$H_5 = \frac{1}{2}[e^{-\alpha t} - \frac{1}{D}(H_3 - \kappa_1 H_7)] \ ,$$

$$H_6 = \frac{1}{2D} (\kappa_1 H_8 - H_4) \ ,$$

$$H_7 = d_2 d_4(1-2\alpha t)e^{-\alpha t} - d_2 d_3[1-2\alpha(t-h)]e^{-\alpha(t+2h)}$$
$$\qquad + \{2d_2 d_3 \alpha h[1+2\alpha(t-h) - d_1 d_4\}e^{\alpha(t-2\alpha)} + d_1 d_3 e^{\alpha(t-4h)} \ ,$$

$$H_8 = \{d_4 d_5 [1-2\alpha(t-h)-2d_2 d_5 \alpha h\} e^{-\alpha t}$$
$$- d_3 d_5 [1-2\alpha(t-h)] e^{-\alpha(t+2h)} \ ,$$

$$H_9 = \frac{1}{2}[(\kappa_2 - 2\alpha h)H_{11} - \frac{d_6}{Dd_3} H_3 e^{2\alpha h}] \ ,$$

$$H_{10} = \frac{1}{2}[(\kappa_2 - 2\alpha h)H_{12} - \frac{d_6}{Dd_3} H_4 e^{2\alpha h} - \frac{d_2}{d_3} e^{-\alpha(t-2h)}] \ ,$$

$$H_{11} = \frac{d_6}{d_2} (e^{\alpha t} + \frac{1}{D} H_7) \ ,$$

$$H_{12} = \frac{d_3}{d_2} [1-2\alpha(t-h)] e^{-\alpha(t-2h)} + \frac{d_6}{d_2 D} H_8 \ , \tag{A5-A16}$$

$$D = -d_2 d_4 + [d_1 d_4 + d_2 d_3 (1+4h^2 \alpha^2)] e^{-2\alpha h} - d_1 d_3 e^{-4\alpha h} \ , \tag{A17}$$

$$d_1 = m\kappa_2 - \kappa_1, \ d_2 = m\kappa_2 + 1, \ d_3 = m-1, \ d_4 = m+\kappa_1, \ d_5 = \kappa_2 + 1 \ ,$$

$$d_6 = m(\kappa_1 + 1), \ m = \mu_1/\mu_2 \ . \tag{A18}$$

APPENDIX B

The generalized Cauchy kernels that appear in equations (86) and (87).

$$k_{31}^{S}(y,s) = -\frac{A(h-s)}{(h-s)^2+y^2} + \frac{B(h-s)][3y^2-(h-s)^2]}{[(h-s)^2+y^2]^2} \quad , \tag{B1}$$

$$k_{32}^{S}(y,s) = \frac{B(s-h)}{(s-h)^2+y^2} + \frac{A(s-h)[3y^2-(s-h)^2]}{[(s-h)^2+y^2]^2} \quad , \tag{B2}$$

$$k_{41}^{S}(y,s) = \frac{Ay}{(h-s)^2+y^2} + \frac{By[y^2-3(h-s)^2]}{[(h-s)^2+y^2]^2} \quad , \tag{B3}$$

$$k_{42}^{S}(y,s) = \frac{By}{(s-y)^2+y^2} + \frac{Ay[y^2-3(s-h)^2]}{[(s-y)^2+y^2]^2} \quad , \tag{B4}$$

$$A = \frac{m(\kappa_2+1)}{m\kappa_2+1} \quad , \quad B = \frac{m(\kappa_2+1)}{m+\kappa_1} \quad , \quad m = \mu_1/\mu_2 \tag{B5}$$

List of Symbols

a_i, b_i:	Crack tip locations, $i=1,2$
c_i:	Specific heat, $i=1,2$
D_i:	Coefficient of thermal diffusivity, $i=1,2$
E_i:	Modulus of elasticity, $i=1,2$
h:	Thickness of the layer
$k_1(a_i), k_1(b_i)$:	Stress intensity factors at the crack tips, $i=1,2$
k_0:	Normalizing stress intensity factor
k_i':	Coefficient of heat conduction, $i=1,2$
t:	time
t_0:	Ramp duration
T_0:	Surface temperature for $t>t_0$
T_∞:	Initial temperature
$T_i(x,t)$:	Temperature, $i=1,2$
u_i, v_i:	Components of the displacement vector, $i=1,2$
x,y,z:	Rectangular coordinates
α_i:	Coefficient of thermal expansion, $i=1,2$
ν_i:	Poisson's ratio, $i=1,2$
μ_i, κ_i:	Elastic constants, $\mu=E/2(1+\nu)$, $\kappa=3-4\nu$ (plane strain)
ρ_i:	Mass density
σ_0:	Normalizing stress, $\sigma_0=-E_1\alpha_1\theta_0/(1-\nu_1)$
σ_{ij}:	Stress components, $(i,j)=(x,y)$
$\theta_i(x,y)$:	Temperature, $\theta_i=T_i-T_\infty$, $i=1,2$; $\theta_0=T_0-T_\infty$
τ:	Normalized time (Fourier Number), $\tau=D_1 t/h^2$
τ_0:	Ramp duration, $\tau_0=D_1 t_0/h^2$
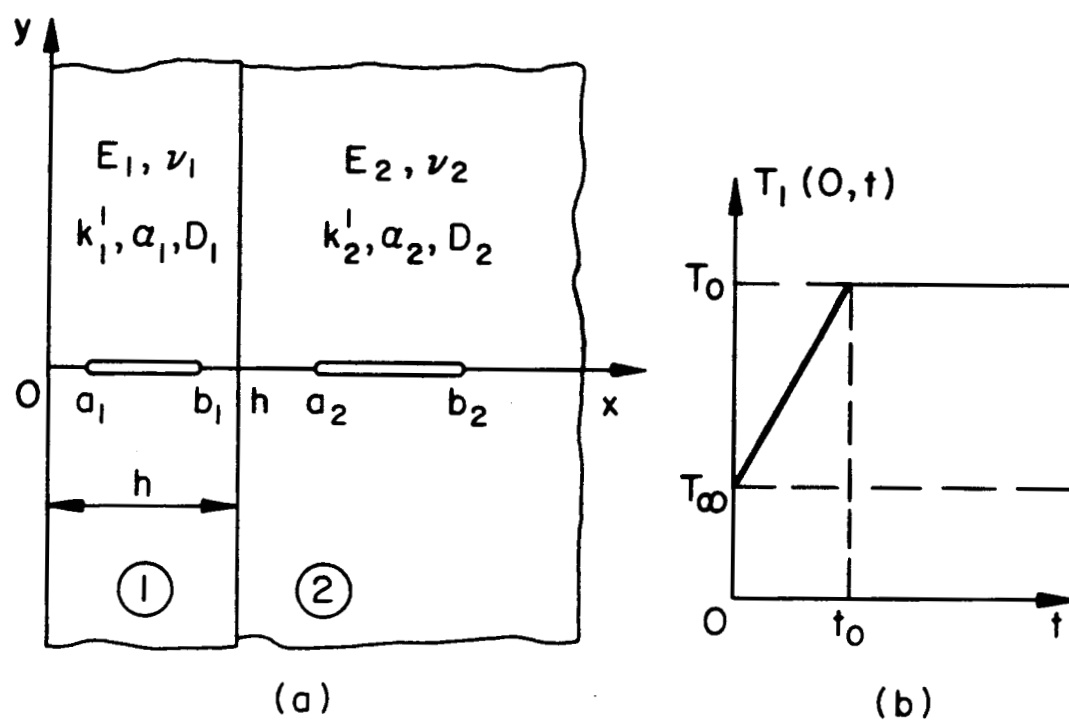
Fig. 1   The crack geometry and the temperature boundary condition
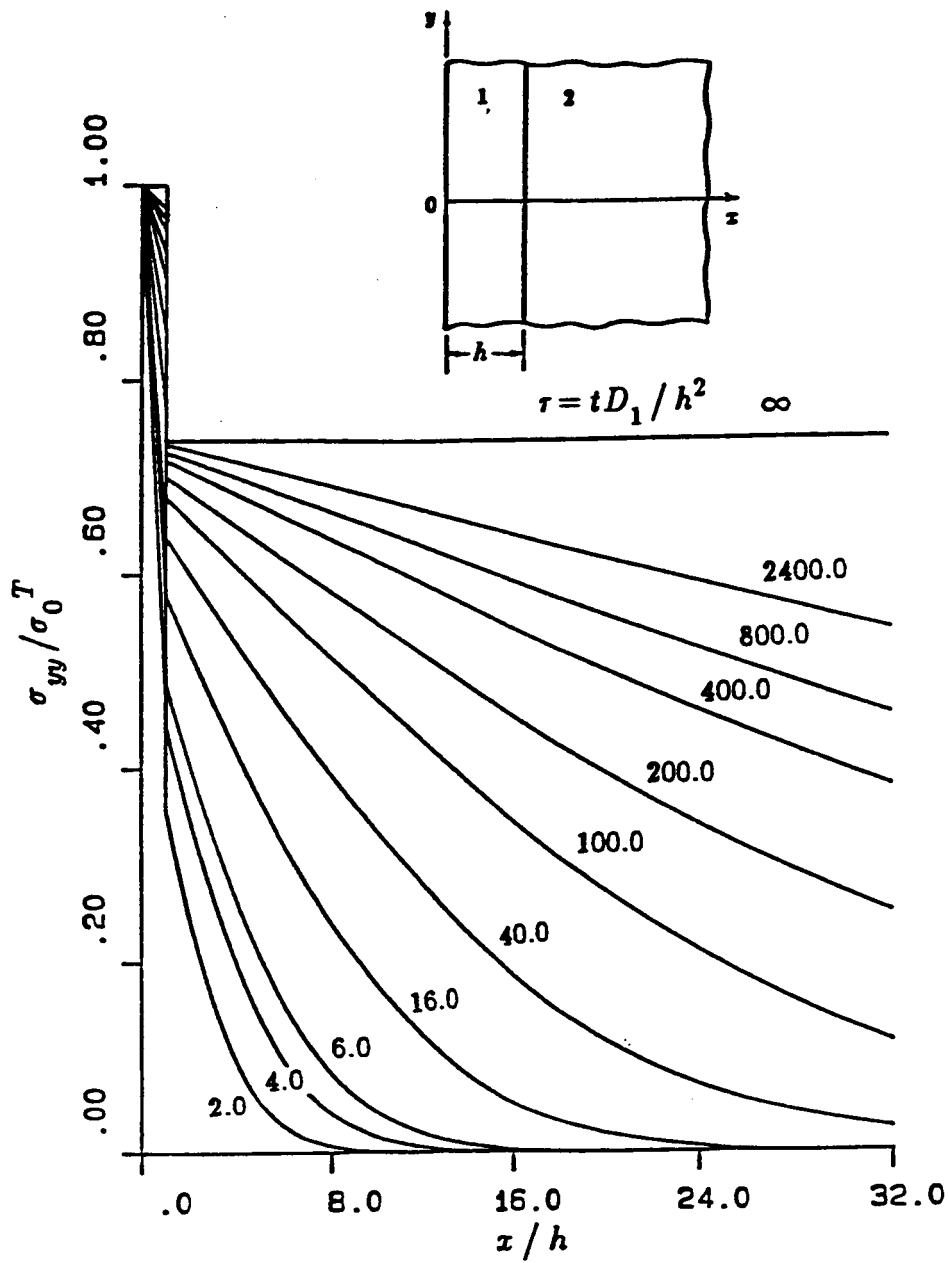
Fig. 2   The normalized transient thermal stress $\sigma_{yy}^{T}(x,t)/\sigma_0$ in the
medium for $\dot{\tau}_0=0$; $(\sigma_0=-E_1\alpha_1\theta_0/(1-\nu_1)$, $\tau=D_1 t/h^2$, $\tau_0=D_1 t_0/h^2$,
material pair A)
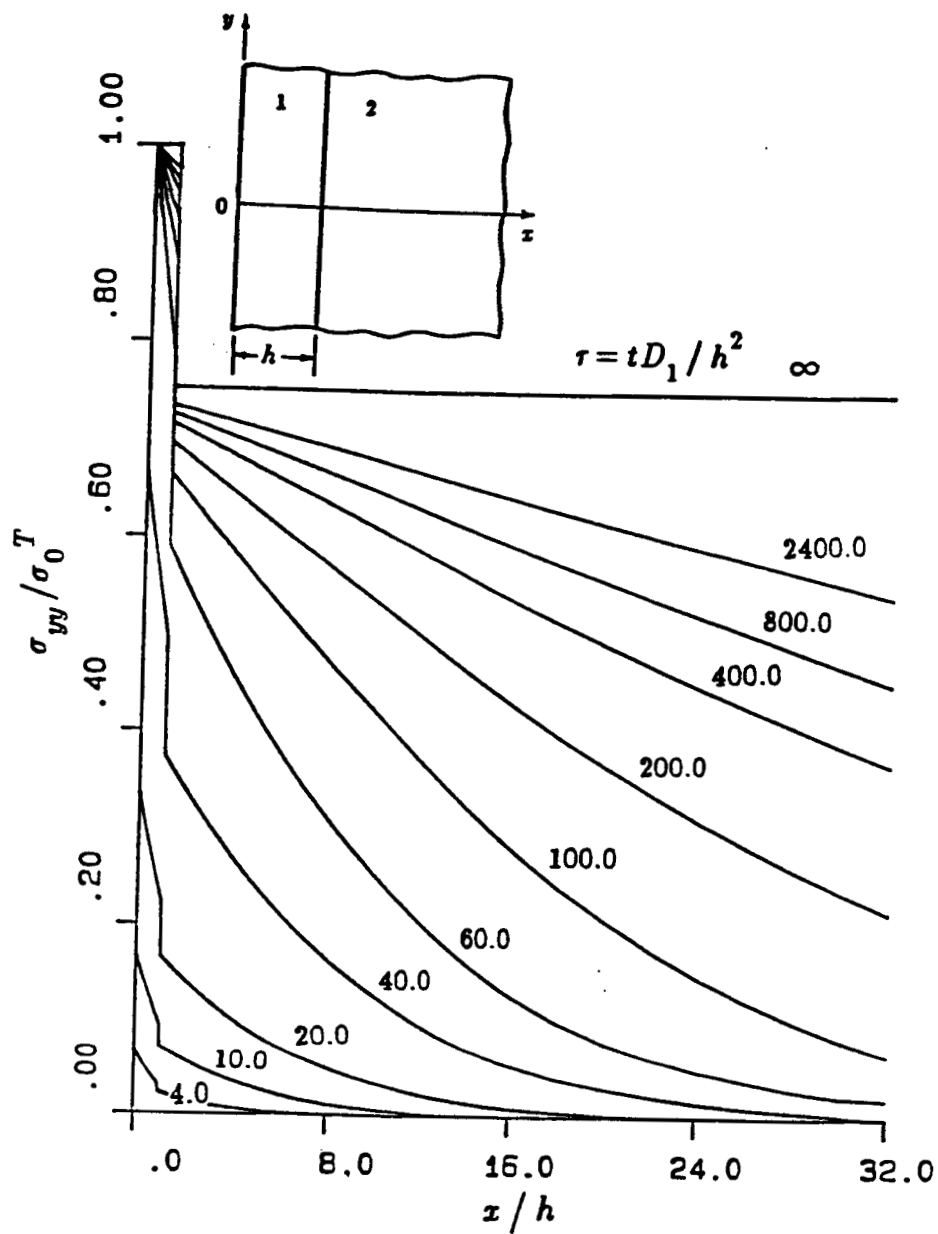
Fig. 3 The normalized stress $\sigma_{yy}^{T}(x,t)/\sigma_0$ for $\tau_0=60$; ($\sigma_0=-E_1\alpha_1\theta_0/(1-\nu_1)$, $\tau=D_1t/h^2$, material pair A)
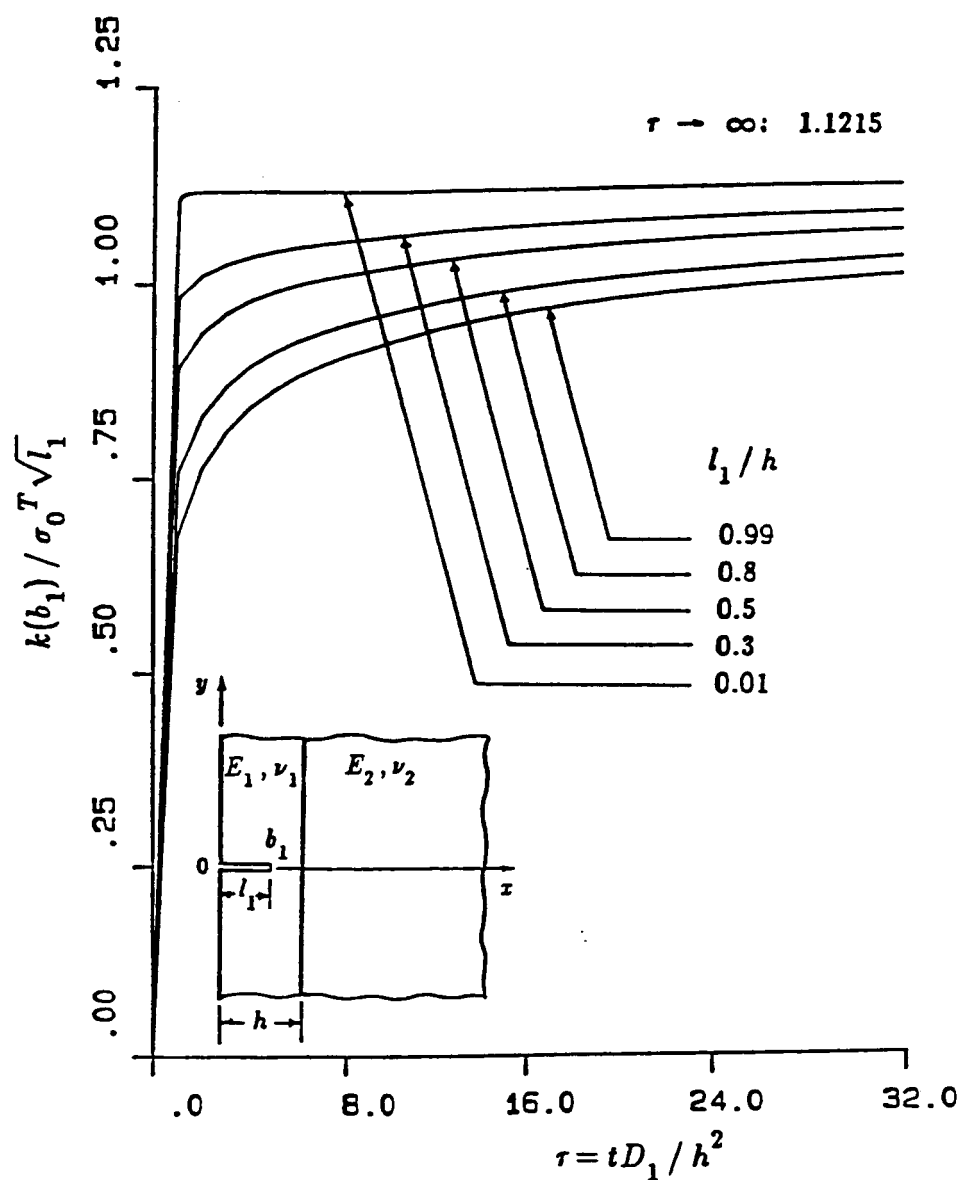
Fig. 4   The normalized stress intensity factor $k_1(b_1)/\sigma_0^T\sqrt{\ell_1}$ in the medium with an edge crack for $\tau_0=0$; ($\ell_1=b_1$, $a_1=0$, $a_2=b_2$, material pair A)
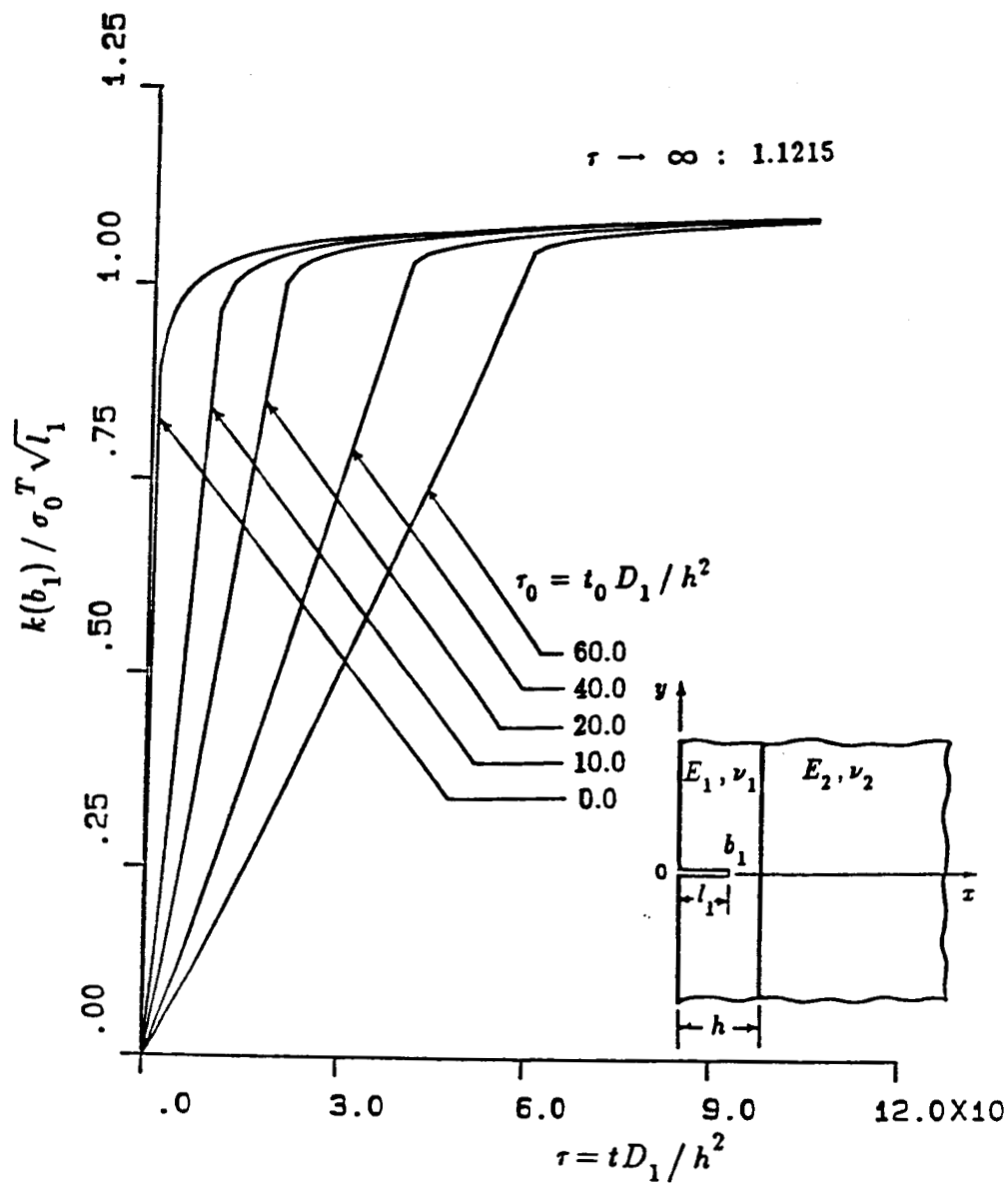
Fig. 5   The influence of the ramp duration τ_0 on the normalized stress intensity factor $k_1(b_1)/\sigma_0\sqrt{\ell_1}$ for a fixed crack length $b_1/h = 0.5$; $(\ell_1 = b_1)$, $a_1 = 0$, material pair A)
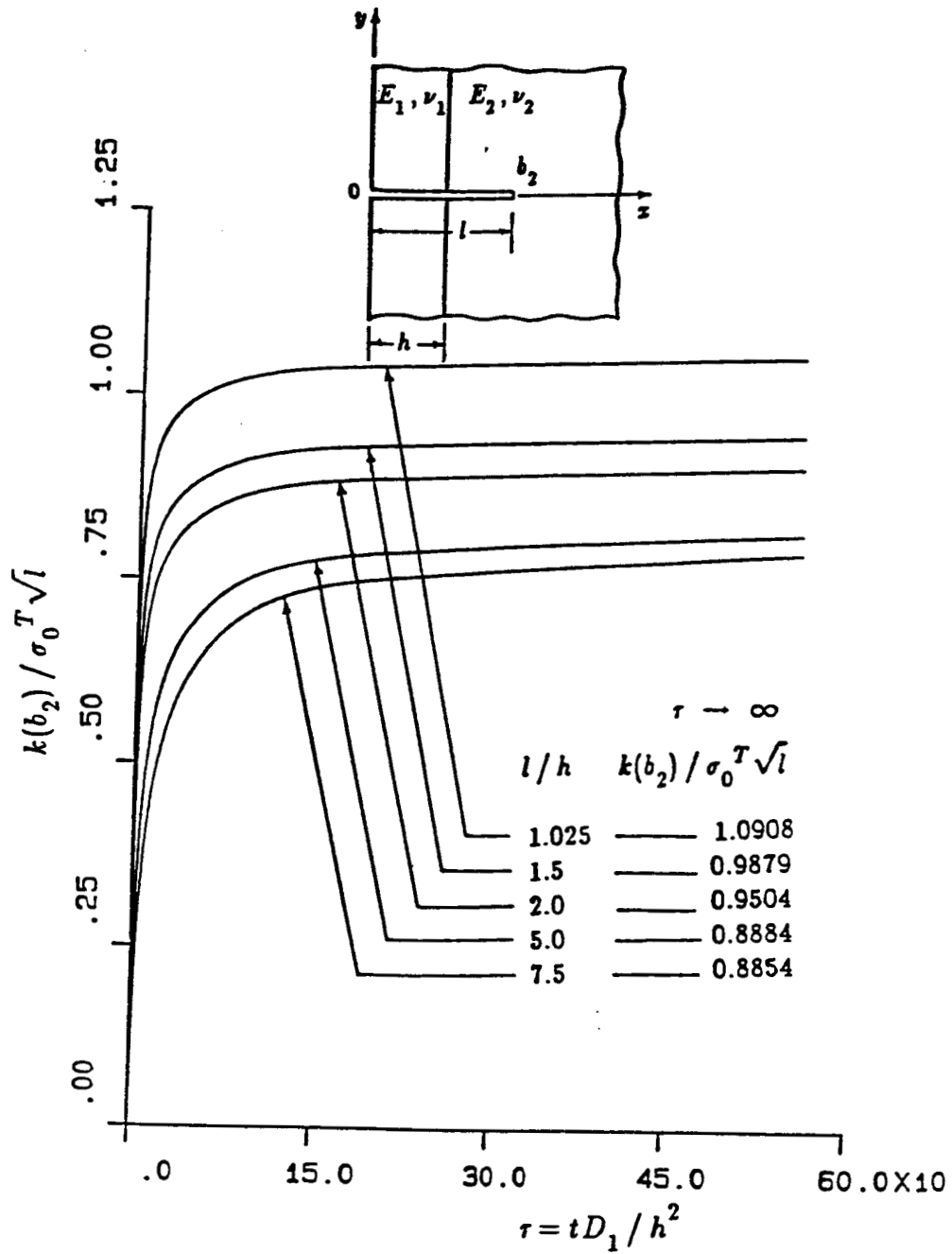
Fig. 6   Normalized stress intensity factor $k_1(b_2)/\sigma_0\sqrt{\ell}$ in the medium with an edge crack crossing the interface for $\tau_0=0$; ($\ell=b_2$, $a_1=0$, $b_1=h=a_2$, material pair A)
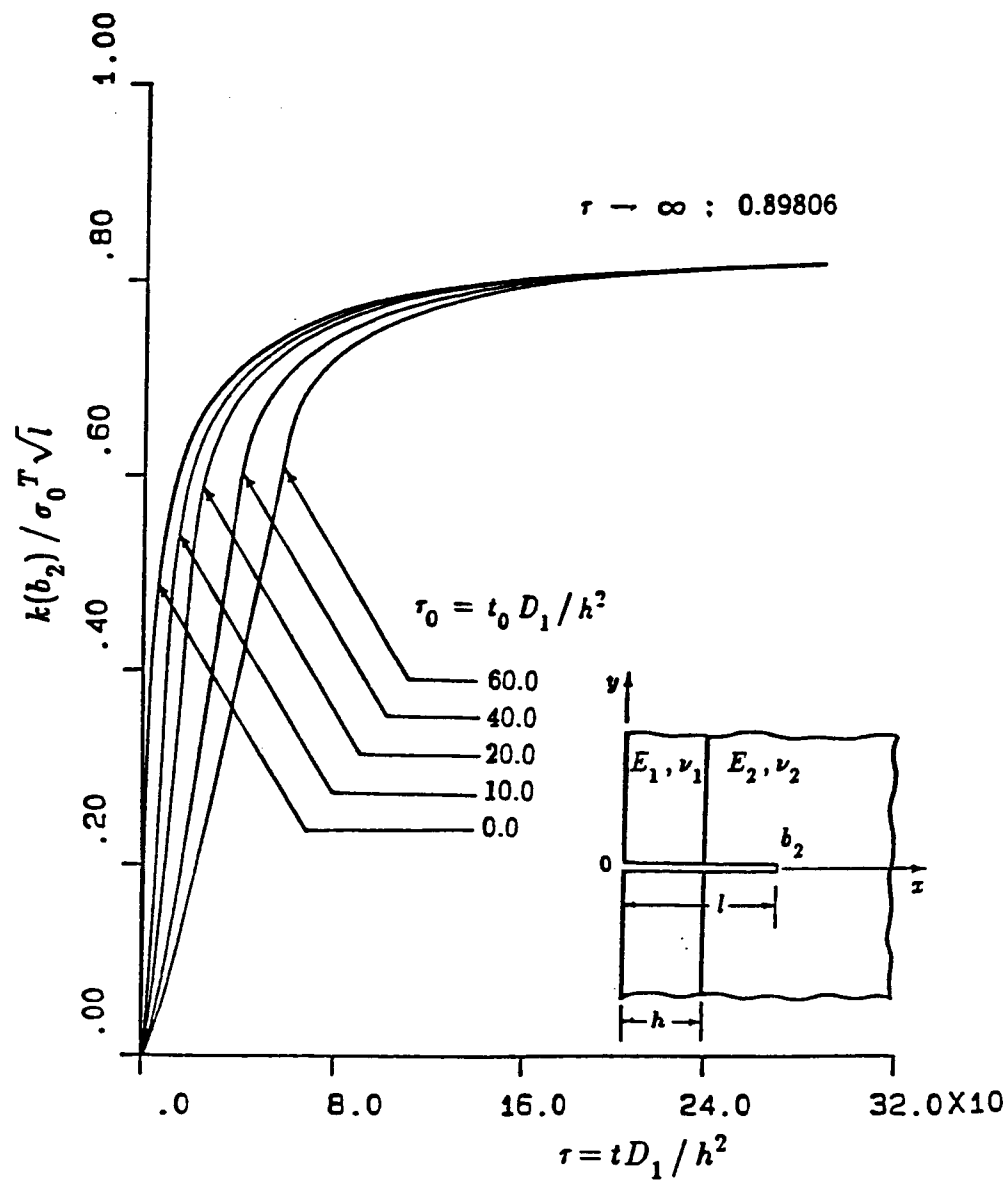
Fig. 7   The influence of surface cooling rate or τ_0 on the normalized
         stress intensity factor $k_1(b_2)/\sigma_0\sqrt{\ell}$ for an edge crack cross-
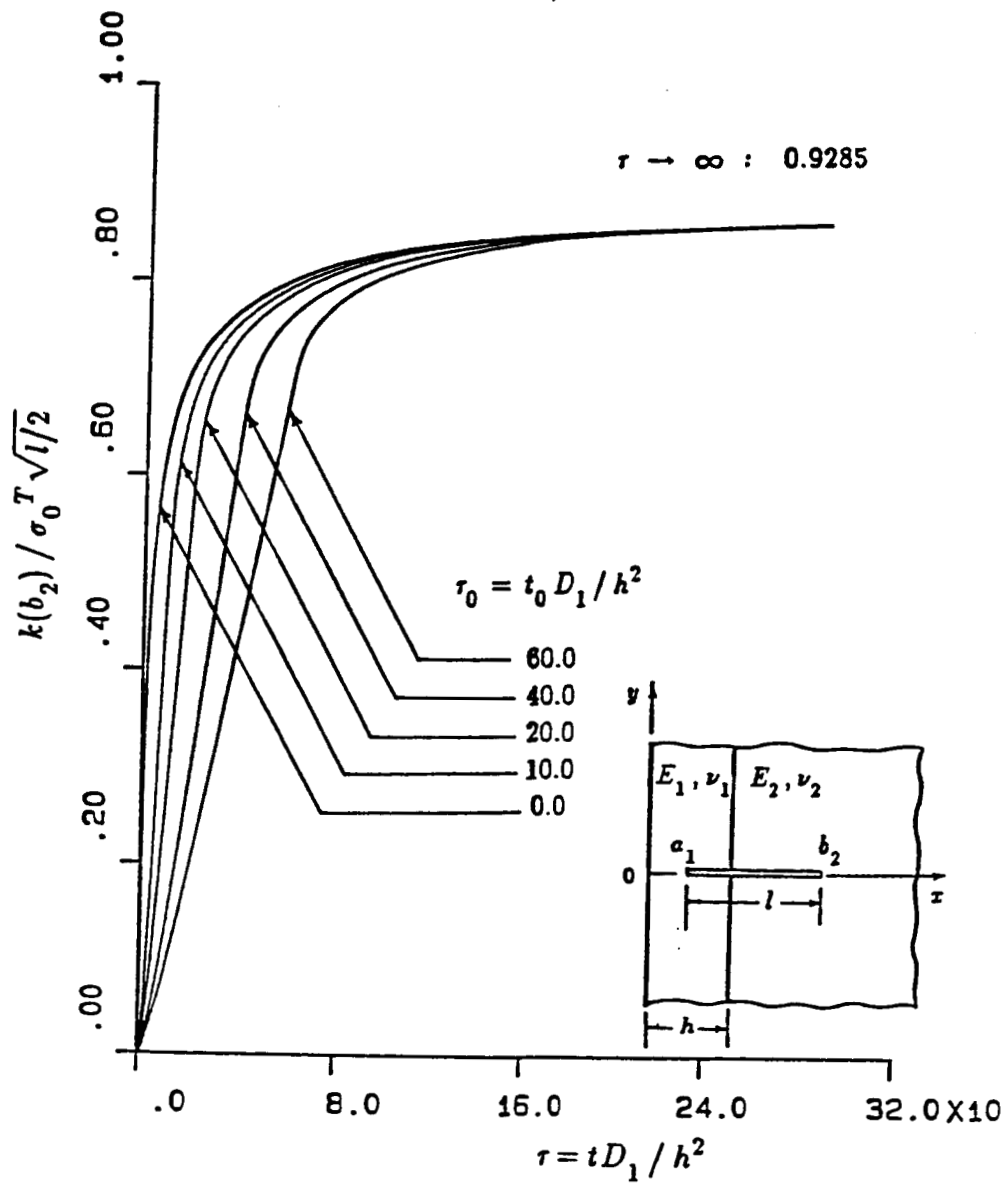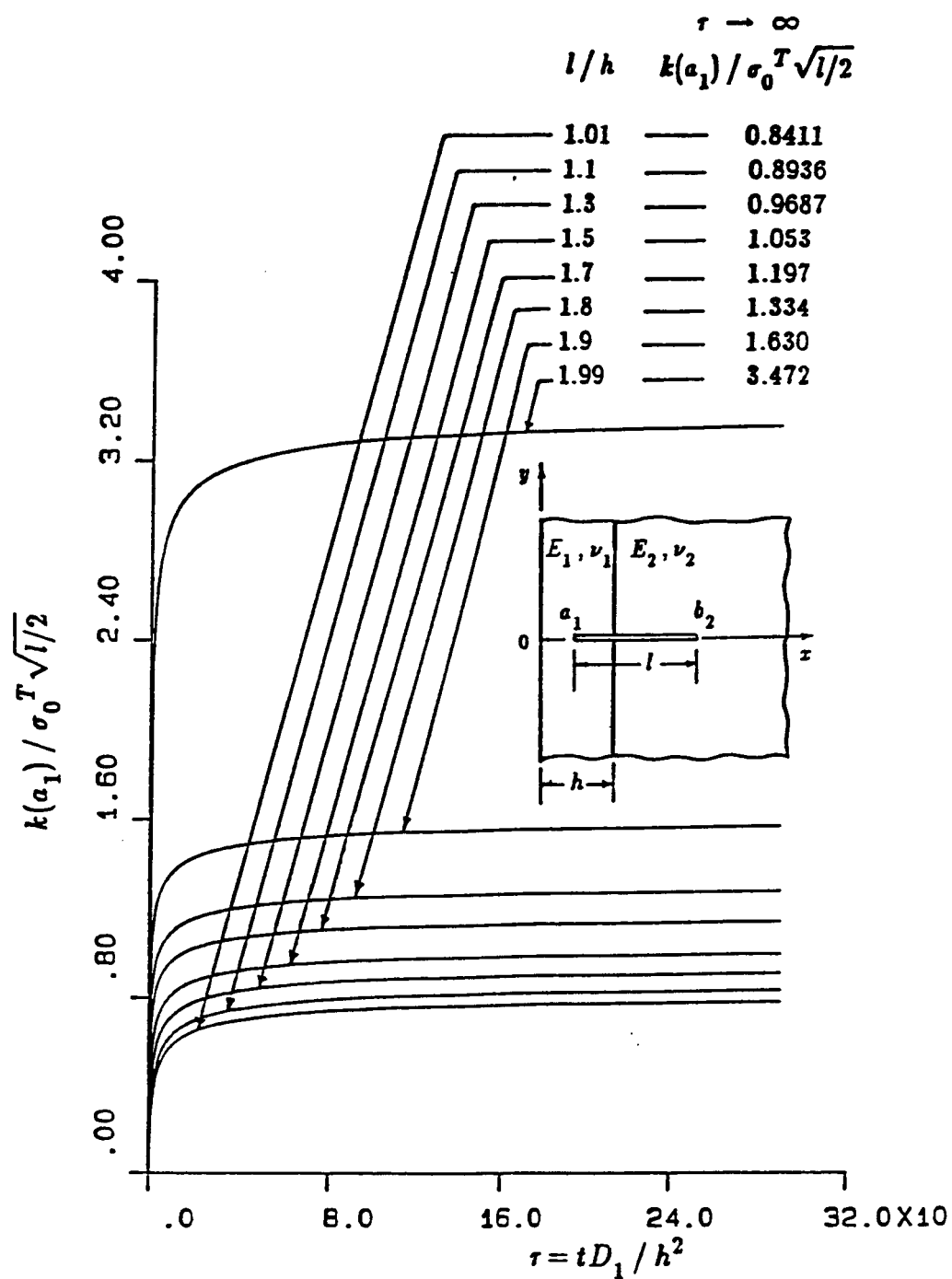   ing the interface; ($\ell=b_2$, $b_2/h=4$, material pair A)
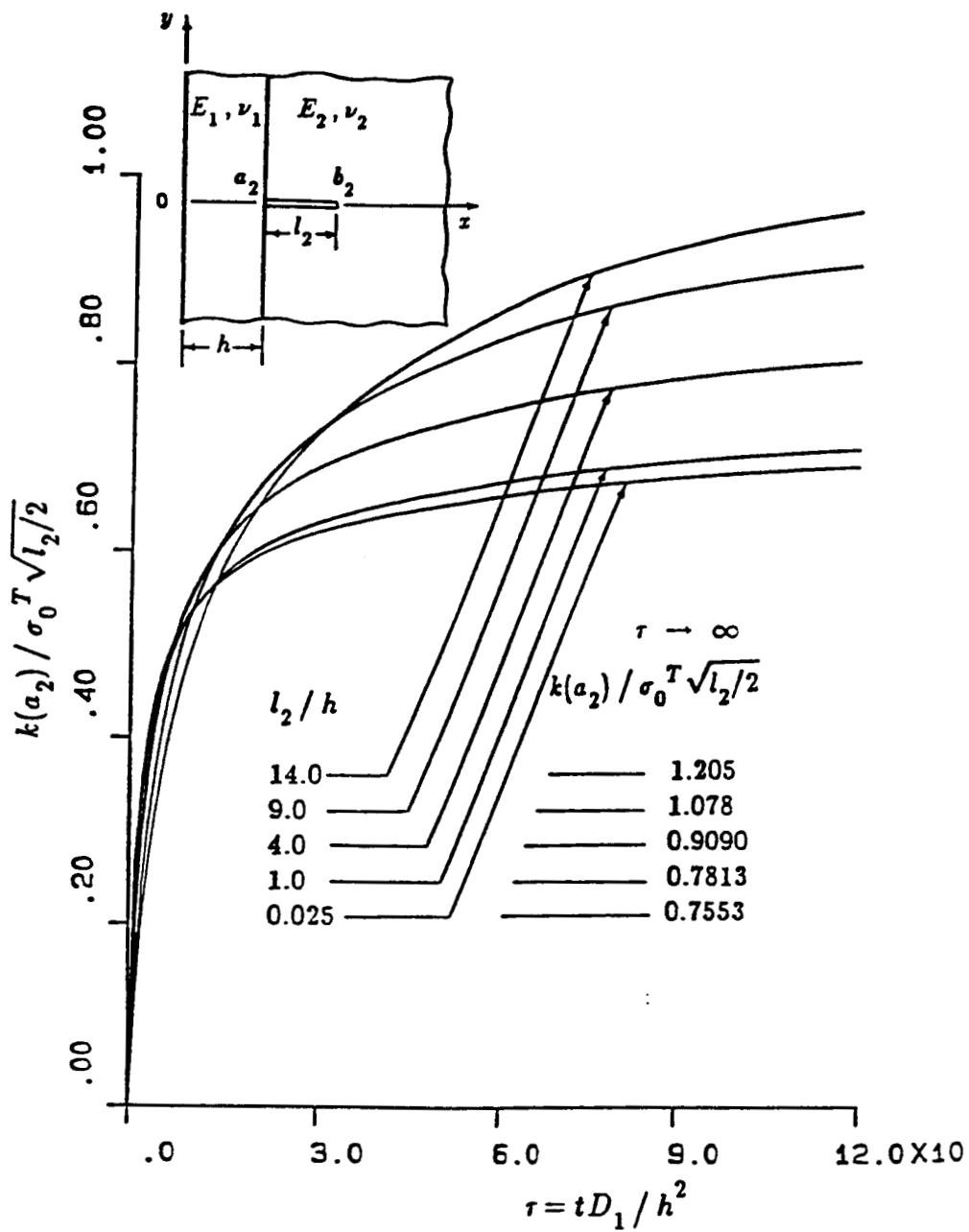
Fig. 8   The normalized stress intensity factor $k_1(a_2)/\sigma_0\sqrt{\ell_2/2}$ in the medium containing an underclad crack for $\tau_0=0$; ($\ell_2=b_2-a_2$, $a_2=h$, $a_1=b_1$, material pair A)
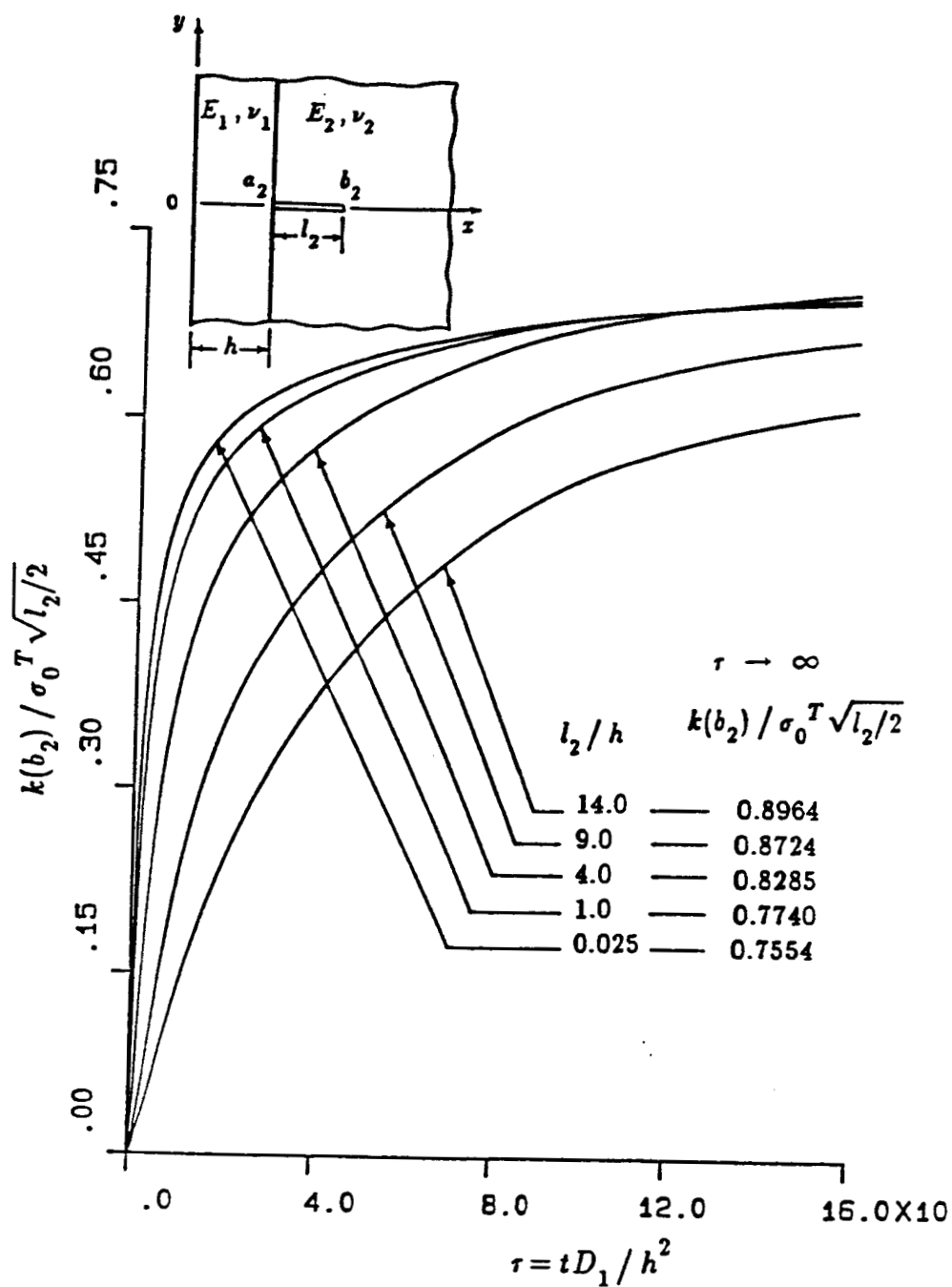
Fig. 9   The normalized stress intensity factor $k_1(b_2)/\sigma_0\sqrt{\ell_2/2}$ in an underclad crack for $\tau_0=0$; ($\ell_2=b_2-a_2$, $a_2=h$, $a_1=b_1$, material pair A)
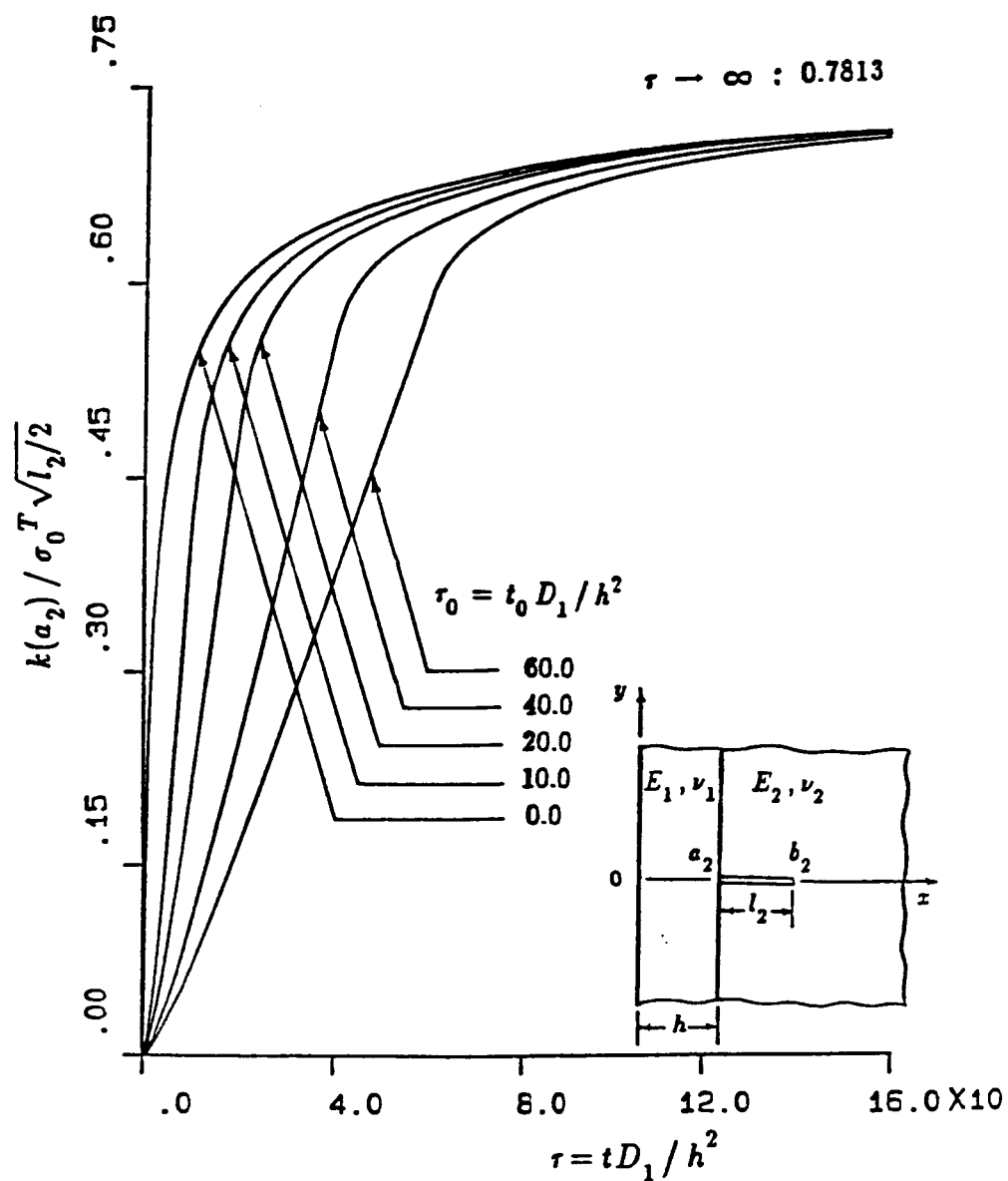
Fig. 10   The influence of τ_0 on the normalized stress intensity factor $k_1(a_2)/\sigma_0\sqrt{\ell_2/2}$ for an underclad crack; ($\ell_2 = b_2 - a_2$, $a_2 = h$, $a_1 = b_1$, material pair A)
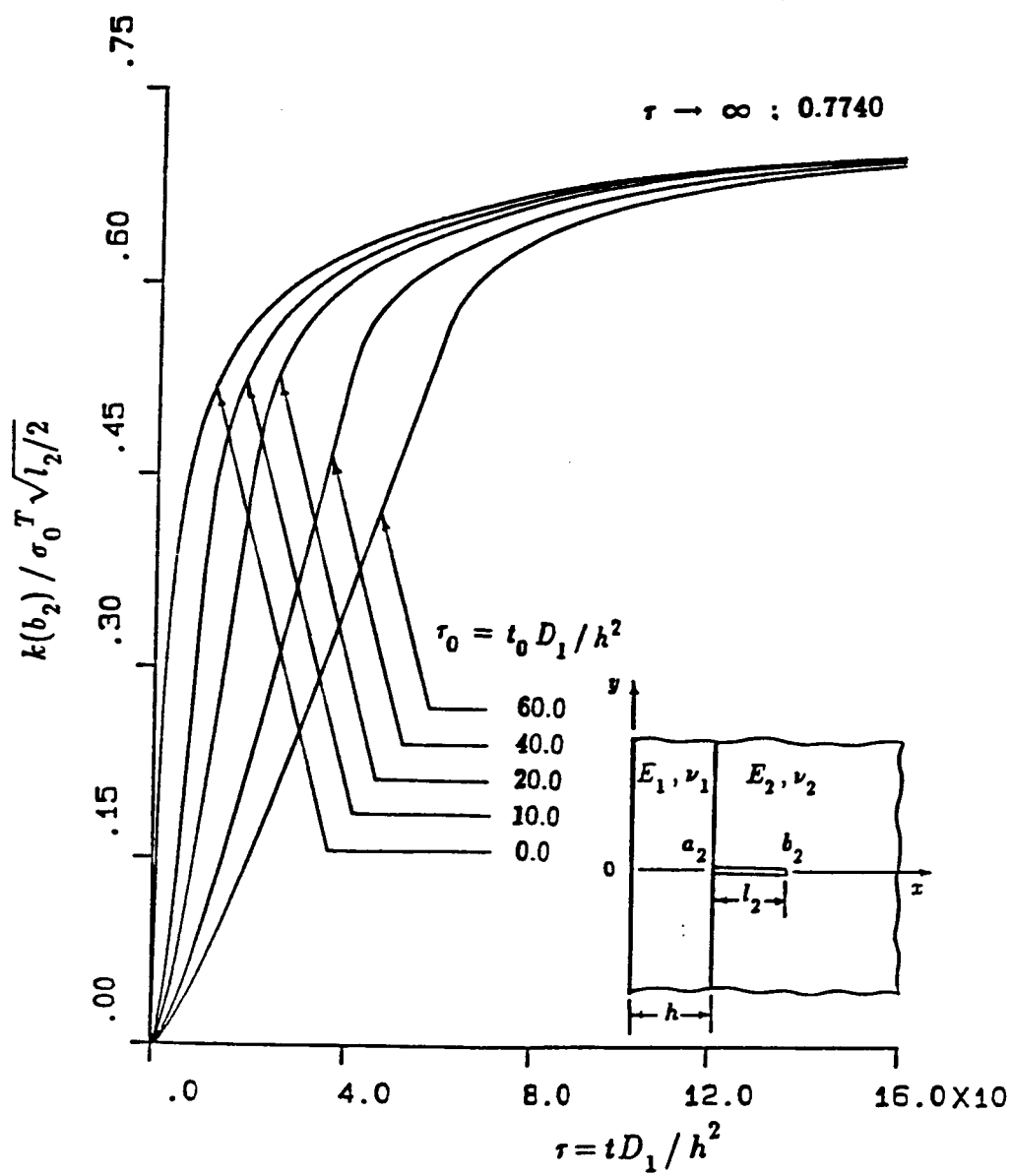
Fig. 11   The influence of τ_0 on $k_1(b_2)/\sigma_0\sqrt{\ell_2/2}$ for an underclad crack;
$(\ell_2=b_2-a_2,\ a_2=h,\ a_1=b_1,\ \text{material pair A})$
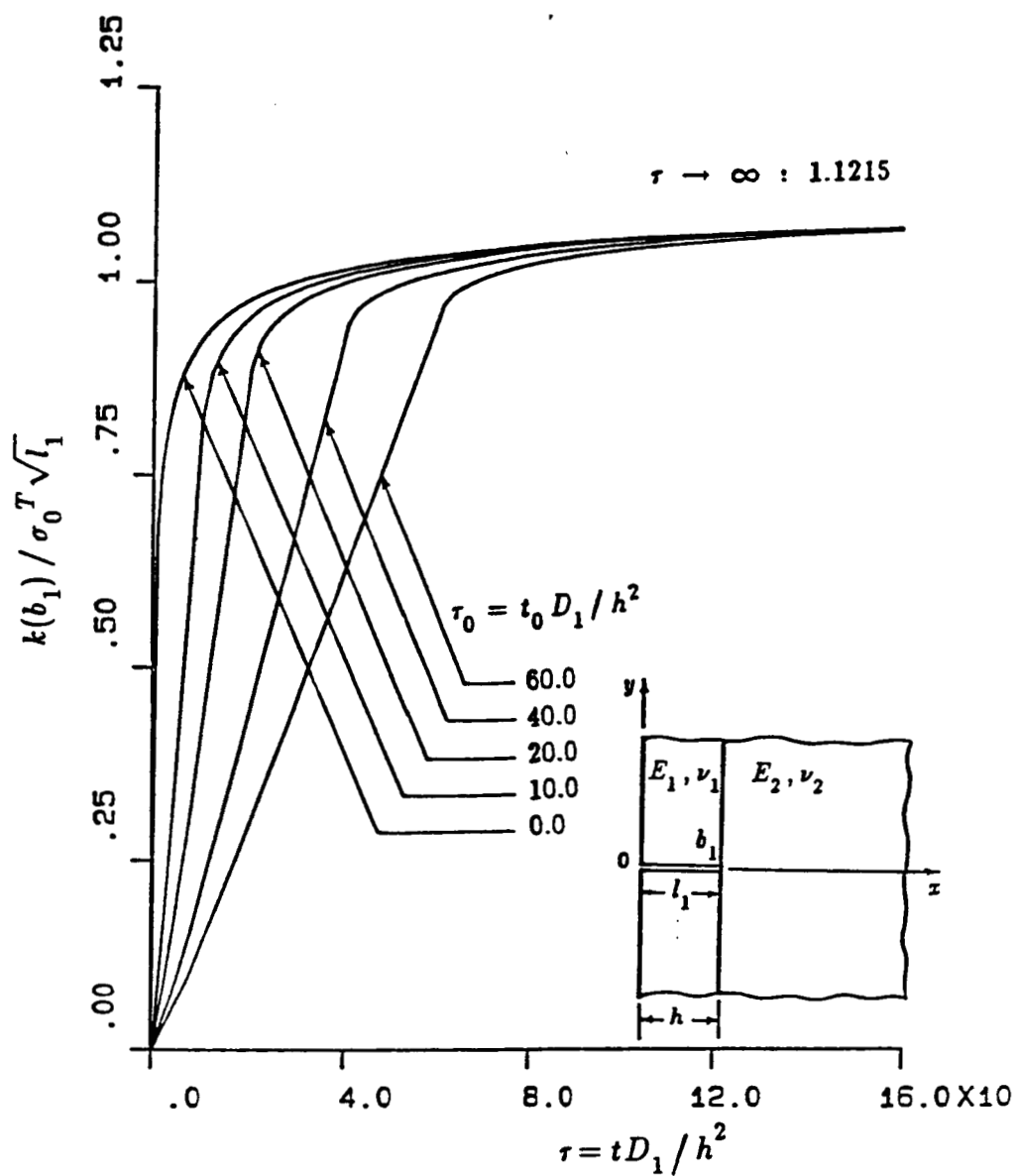
Fig. 12   The normalized stress intensity factor $k(b_1)/\sigma_0\sqrt{\ell_1}$ for broken clad; (a_1=0, ℓ_1=h, b_2=a_2, material pair A)
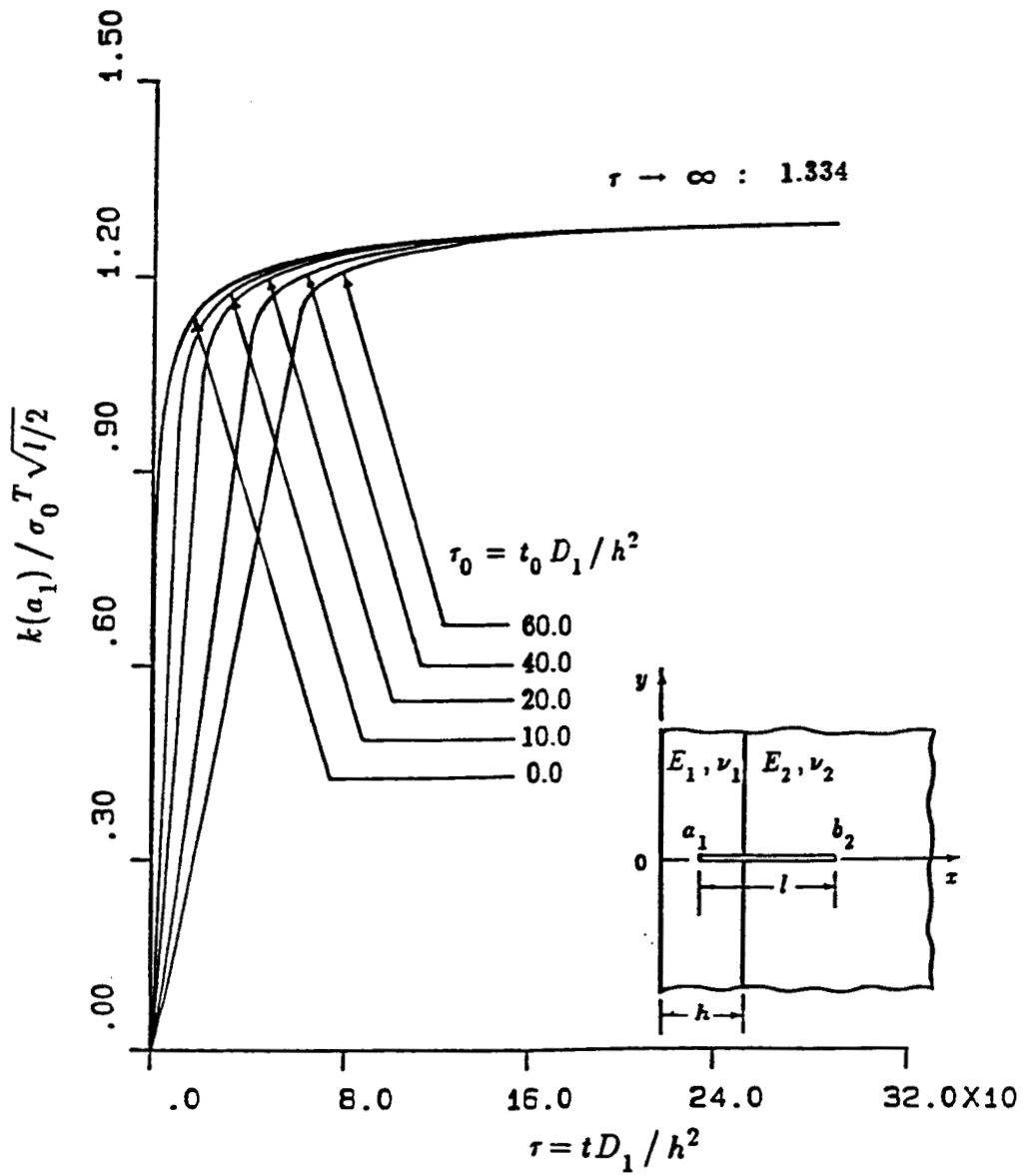
Fig. 13   Influence of τ_0 on the normalized stress intensity factor
$k_1(a_1)/\sigma_0\sqrt{l/2}$ for a crack crossing the interface; ($l=b_2-a_1$,
$a_1/h=0.2$, $b_2/h=2$, material pair A)

$\tau \rightarrow \infty : 0.9285$

$\tau_0 = t_0 D_1 / h^2$

60.0
40.0
20.0
10.0
0.0

$k(b_2) / \sigma_0^T \sqrt{l/2}$

$\tau = tD_1 / h^2$

.0   8.0   16.0   24.0   32.0 X10

Fig. 14   Influence of τ_0 on the normalized stress intensity factor
$k_1(b_2)/\sigma_0\sqrt{l/2}$ for a crack crossing the interface; ($l=b_2-a_1$,
a/h=0.2, b_2/h=2, material pair A)

Fig. 15   The normalized stress intensity factor $k_1(a_1)/\sigma_0\sqrt{\ell/2}$ for an embedded crack crossing the interface; ($\ell=b_2-a_1$, $b_2=2h$, $\tau_0=0$, material pair A)
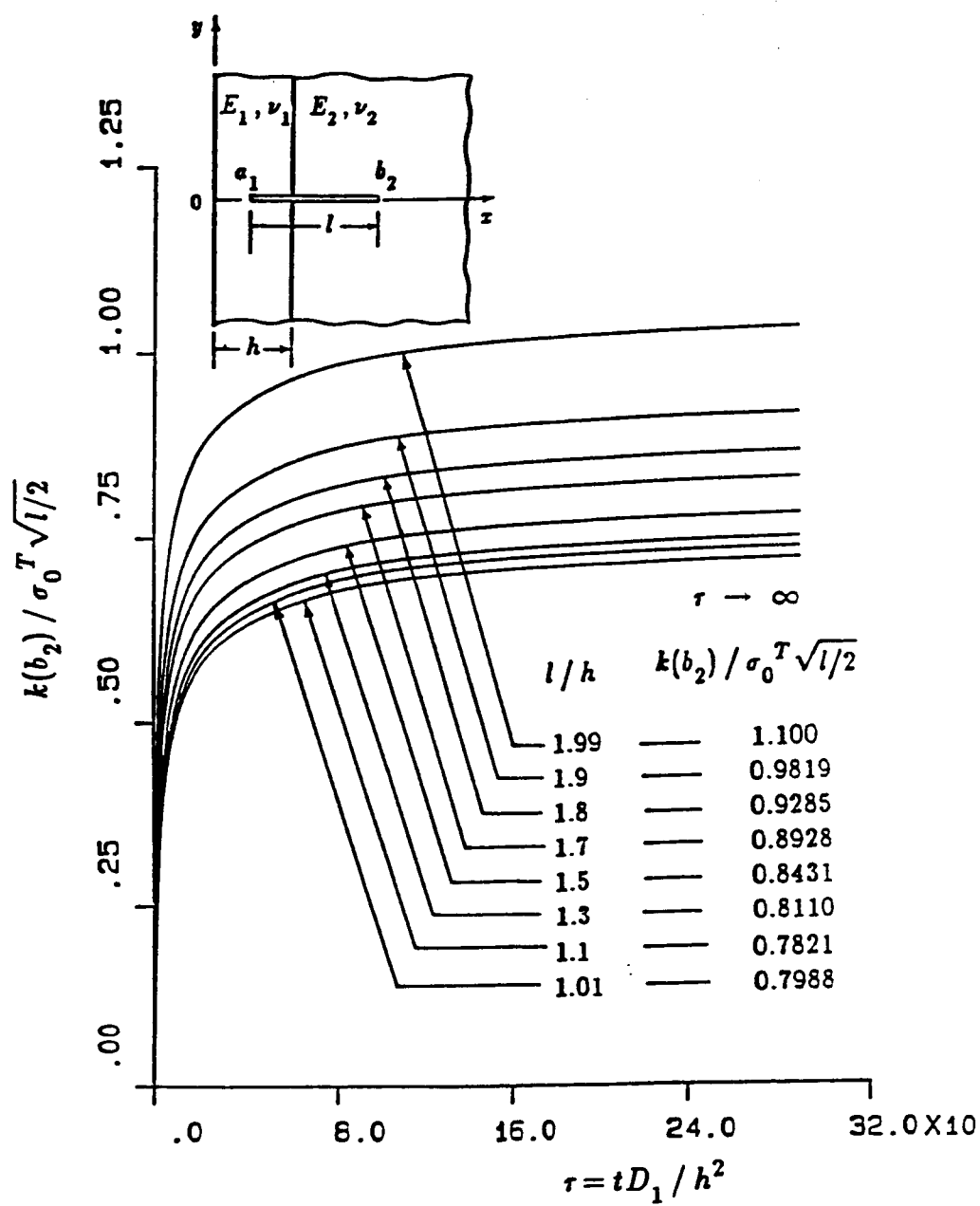
Fig. 16 The normalized stress intensity factor $k_1(b_2)/\sigma_0\sqrt{\ell/2}$ for an
embedded crack crossing the interface; ($\ell=b_2-a_1$, $b_2=2h$,
$\tau_0=0$, material pair A)
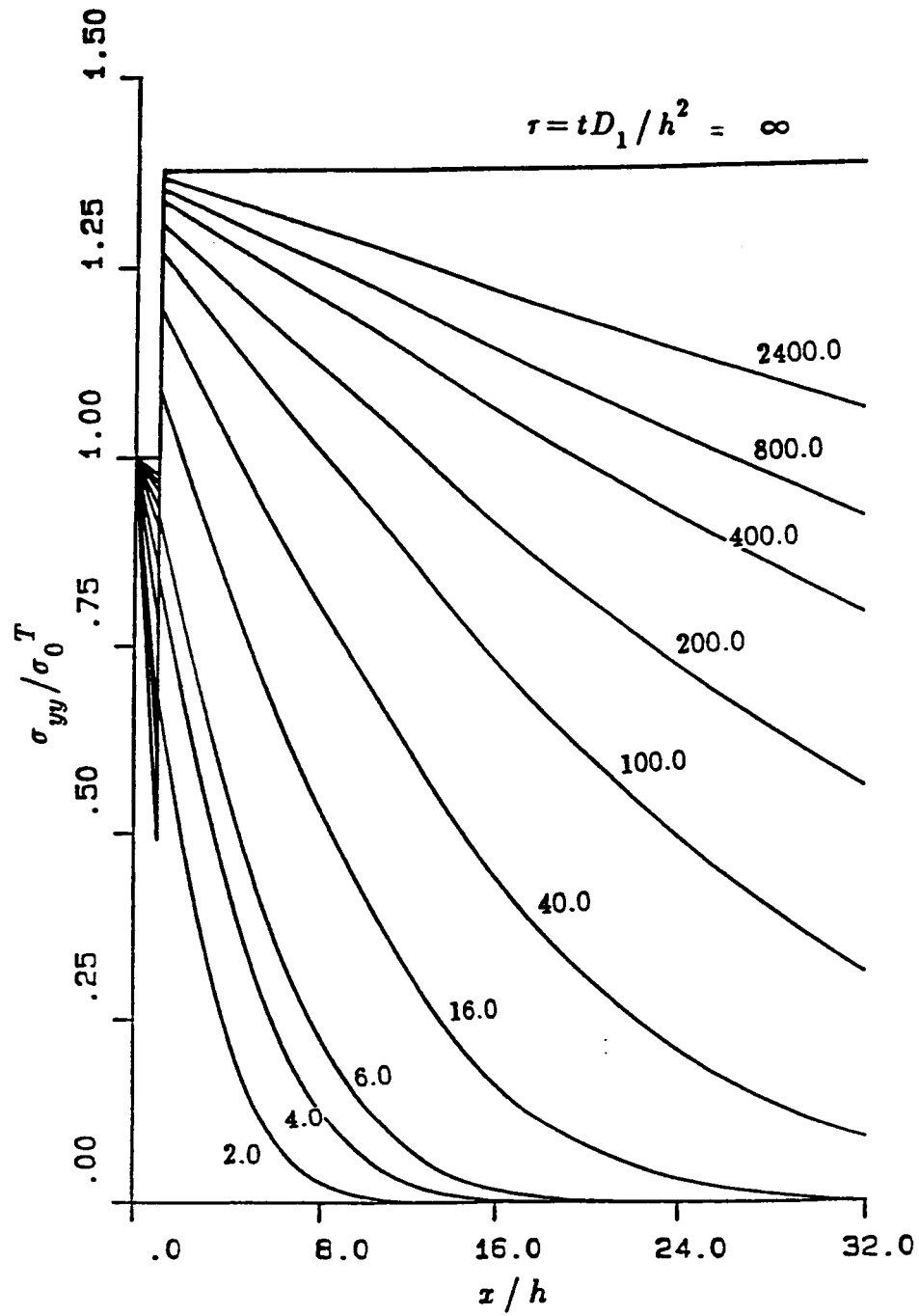
Fig. 17 The normalized transient thermal stress $\sigma_{yy}^{T}(x,t)/\sigma_0$ in material pair B for $\tau_0=0$; ($\sigma_0=-E_1\alpha_1\theta_0/(1-\nu_1)$, $\tau=D_1t/h^2$, $\tau_0=D_1t_0/h^2$)
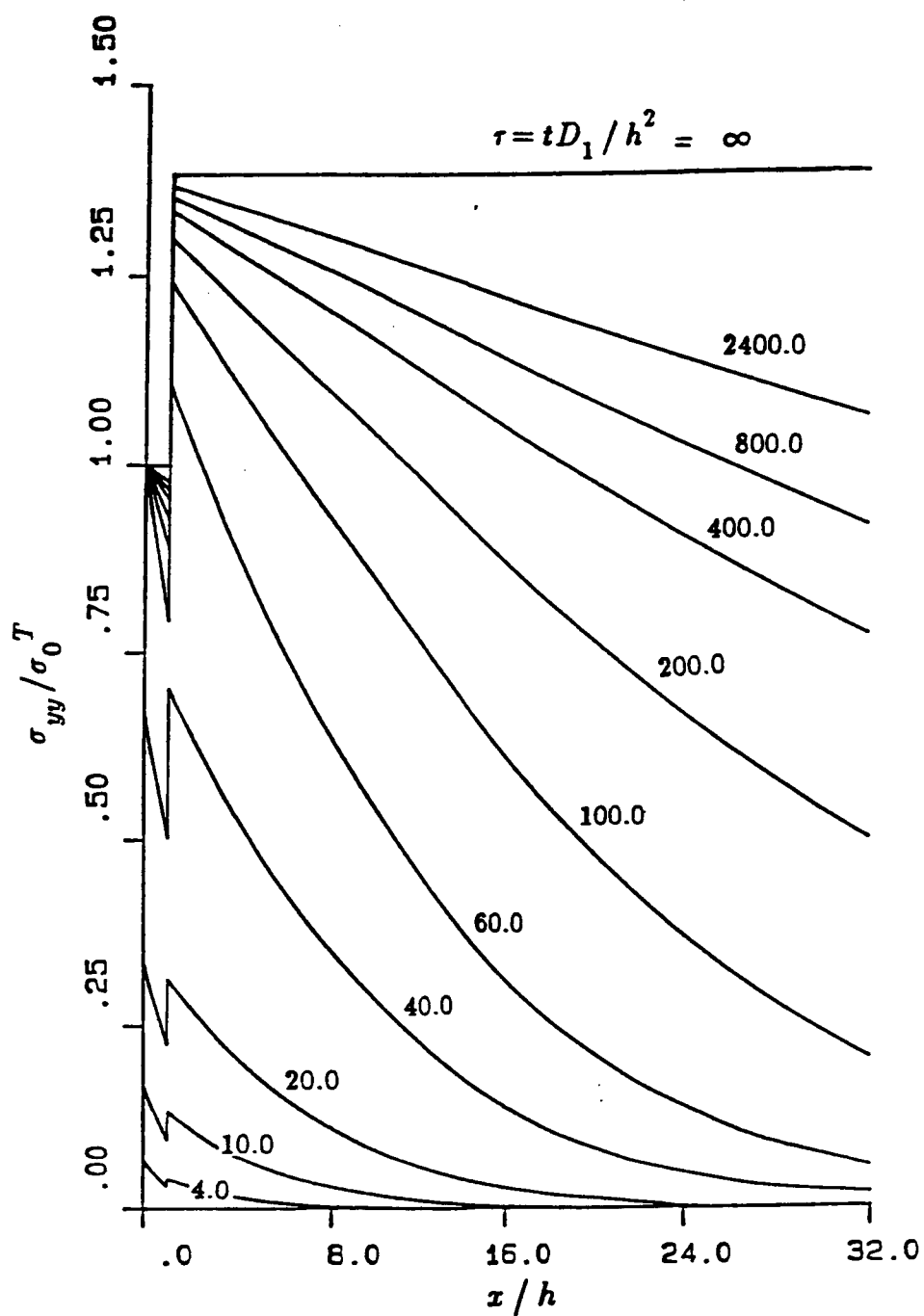
Fig. 18   The normalized thermal stress $\sigma_{yy}^{T}(x,t)/\sigma_{0}$ in material pair
B for $\tau_{0}=60$; $(\sigma_{0}=-E_{1}\alpha_{1}\theta_{0}/(1-\nu_{1})$, $\tau_{0}=D_{1}t_{0}/h^{2})$
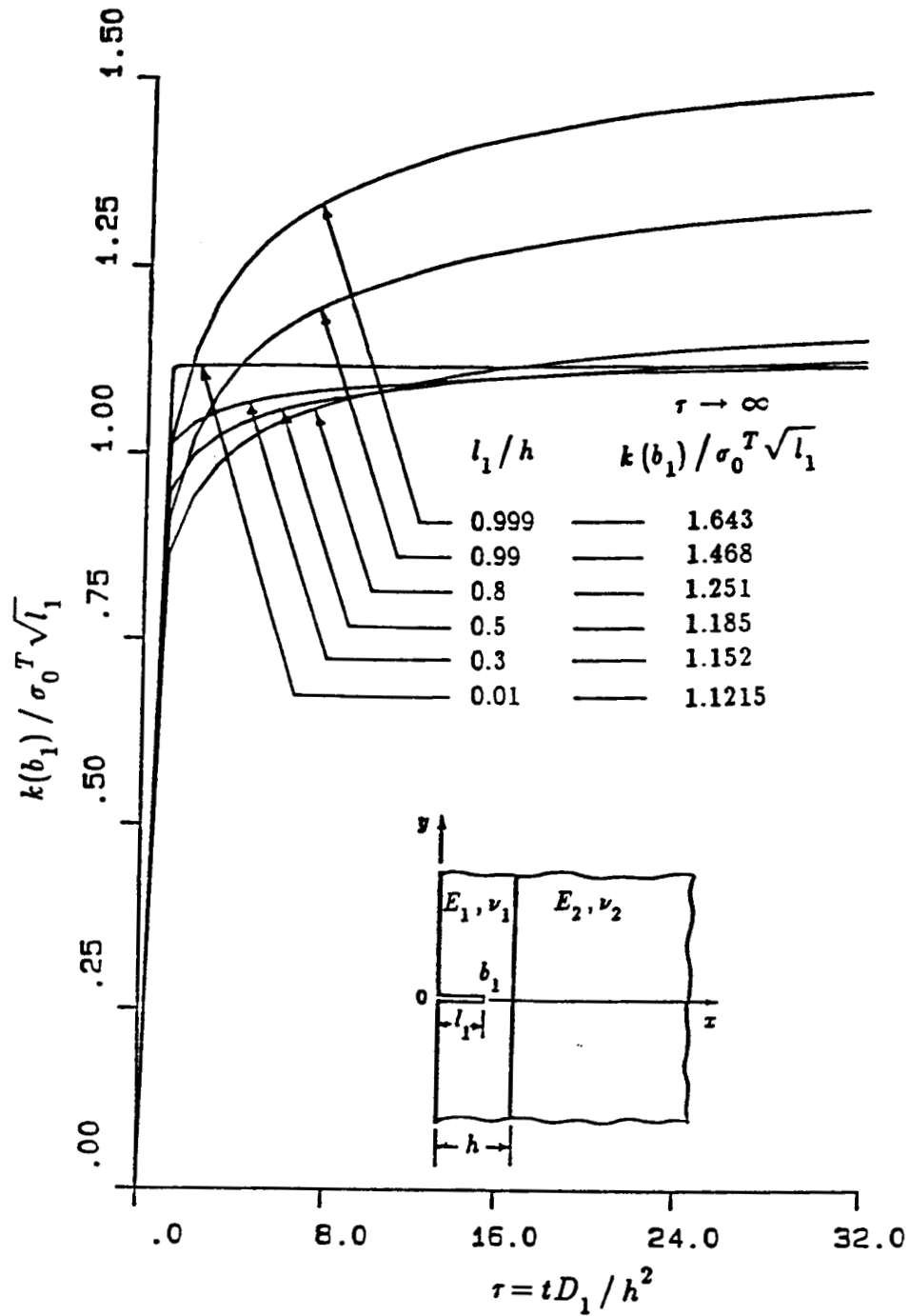
Fig. 19   The normalized stress intensity factor $k_1(b_1)/\sigma_0\sqrt{\ell_1}$ in material pair B with an edge crack; $(\ell_1=b_1,\ a_1=0,\ \tau_0=0,\ b_2=a_2)$

Fig. 20   The influence of τ_0 on the normalized stress intensity factor $k_1(b_1)/\sigma_0\sqrt{\ell_1}$ in material pair B with an edge crack; (ℓ_1=b$_1$, a$_1$=0, b$_1$/h=0.5, a$_2$=b$_2$)
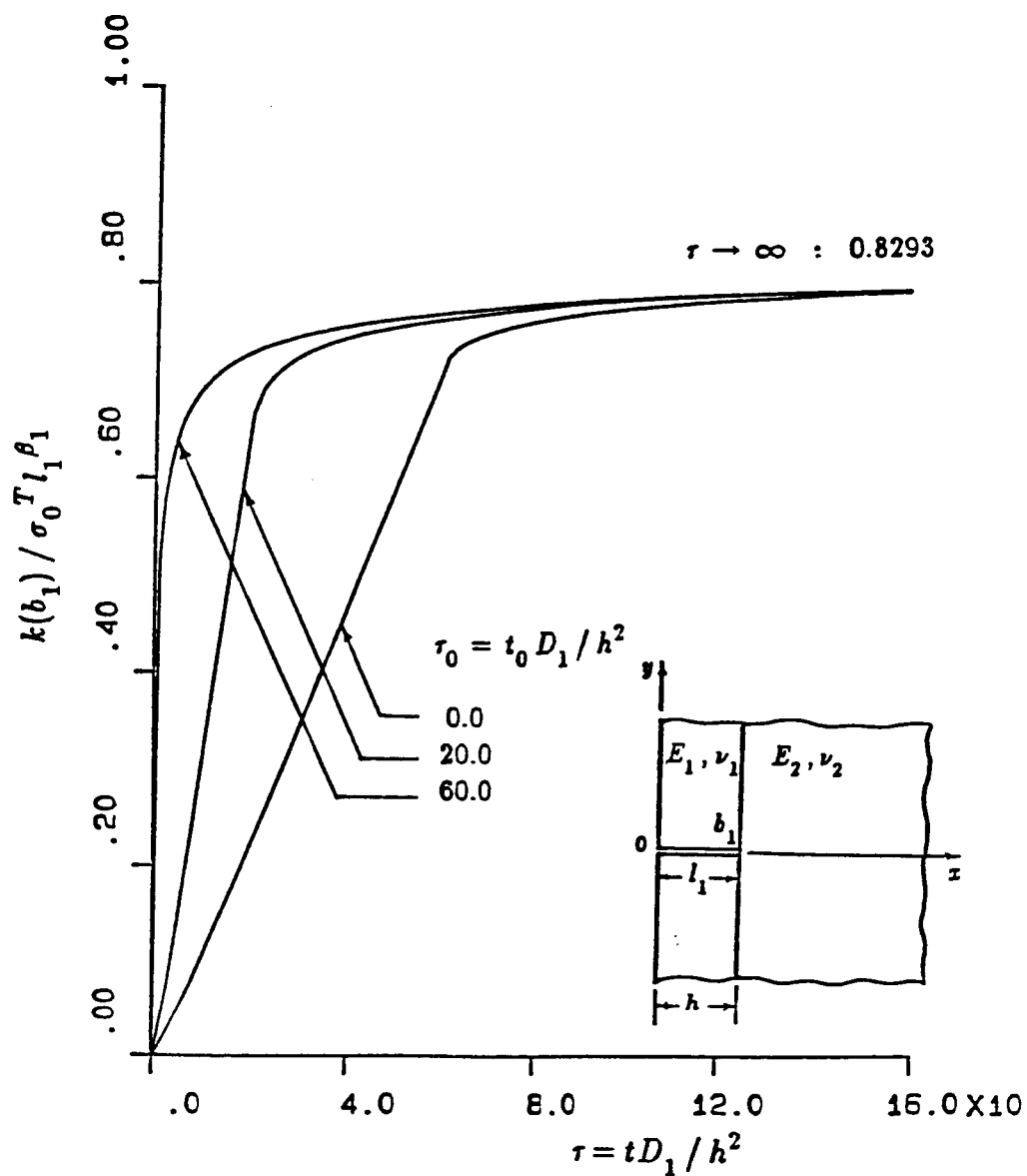
$$\tau \rightarrow \infty \ : \ 0.8293$$

$$\tau_0 = t_0 D_1 / h^2$$

0.0
20.0
60.0

$$\tau = t D_1 / h^2$$

Fig. 21   The influence of τ_0 on the normalized stress intensity factor $k_1(b_1)/\sigma_0 \ell_1^{\beta_1}$ in material pair B with a broken layer; ($a_1=0$, $b_1=h$, $a_2=b_2$, $\sigma_{ij} \sim r^{-\beta_1}$, $\beta_1=0.552538$)
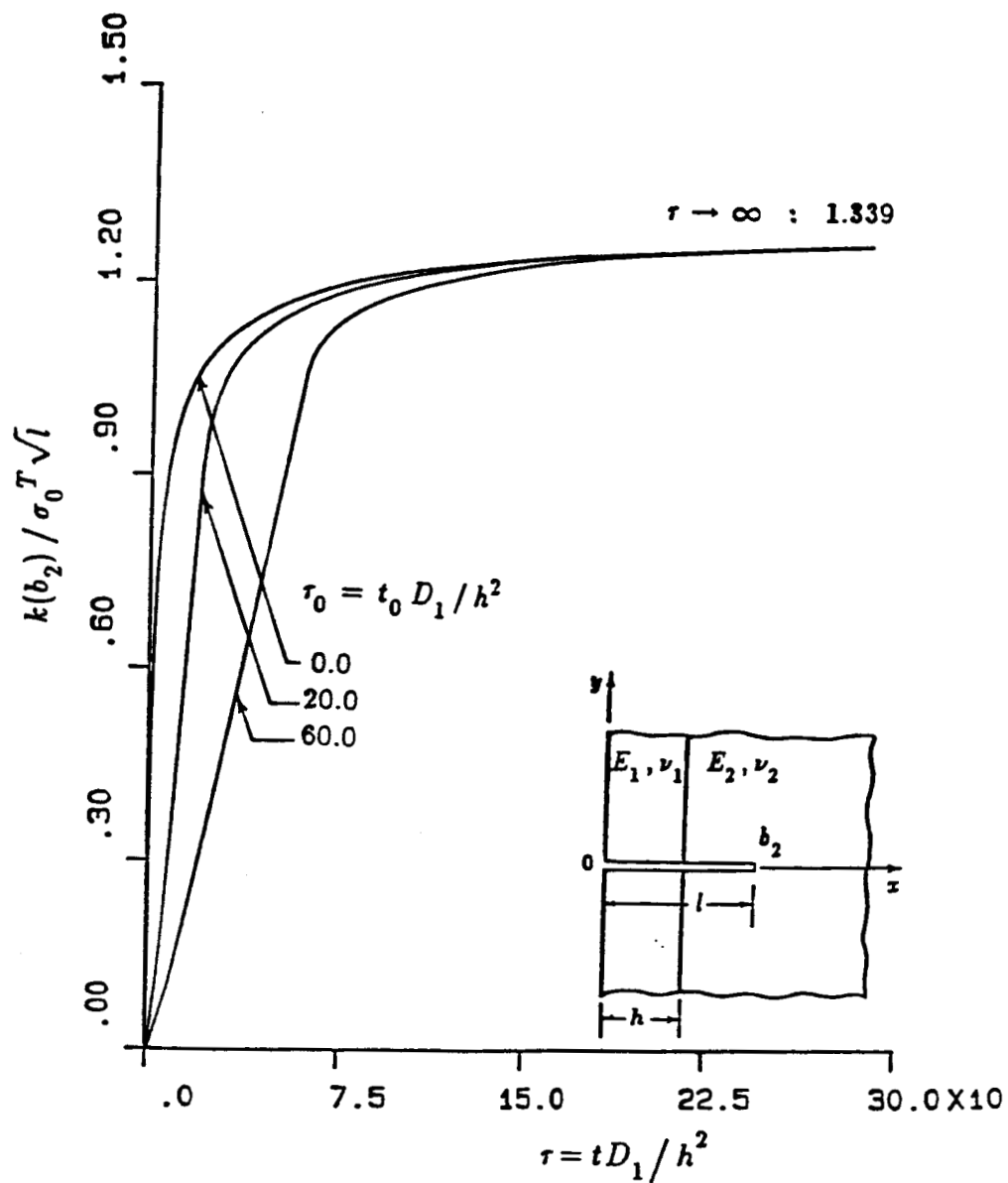
Fig. 22   The influence of τ_0 on the normalized stress intensity factor $k_1(b_2)/\sigma_0\sqrt{\ell}$ in material pair B with an edge crack crossing the interface; ($a_1=0$, $b_1=h=a_2$, $b_2=2h$, $\sigma_0=-E_1\alpha_1\theta_0/(1-\nu_1)$)
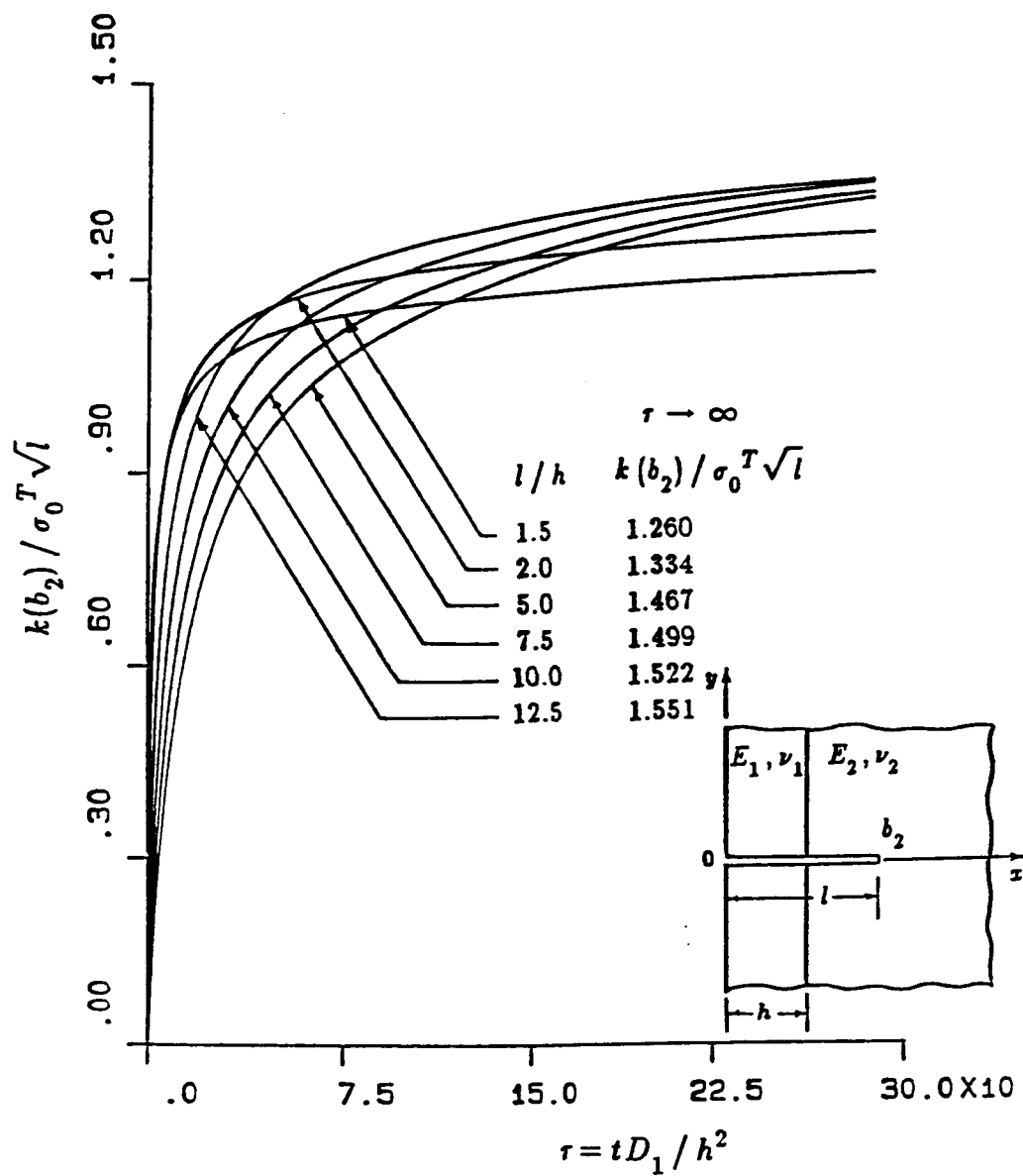
Fig. 23   The normalized stress intensity factor $k_1(b_2)/\sigma_0\sqrt{\ell}$ in material
pair B with an edge crack crossing the interface; (τ_0=0, a_1=0,
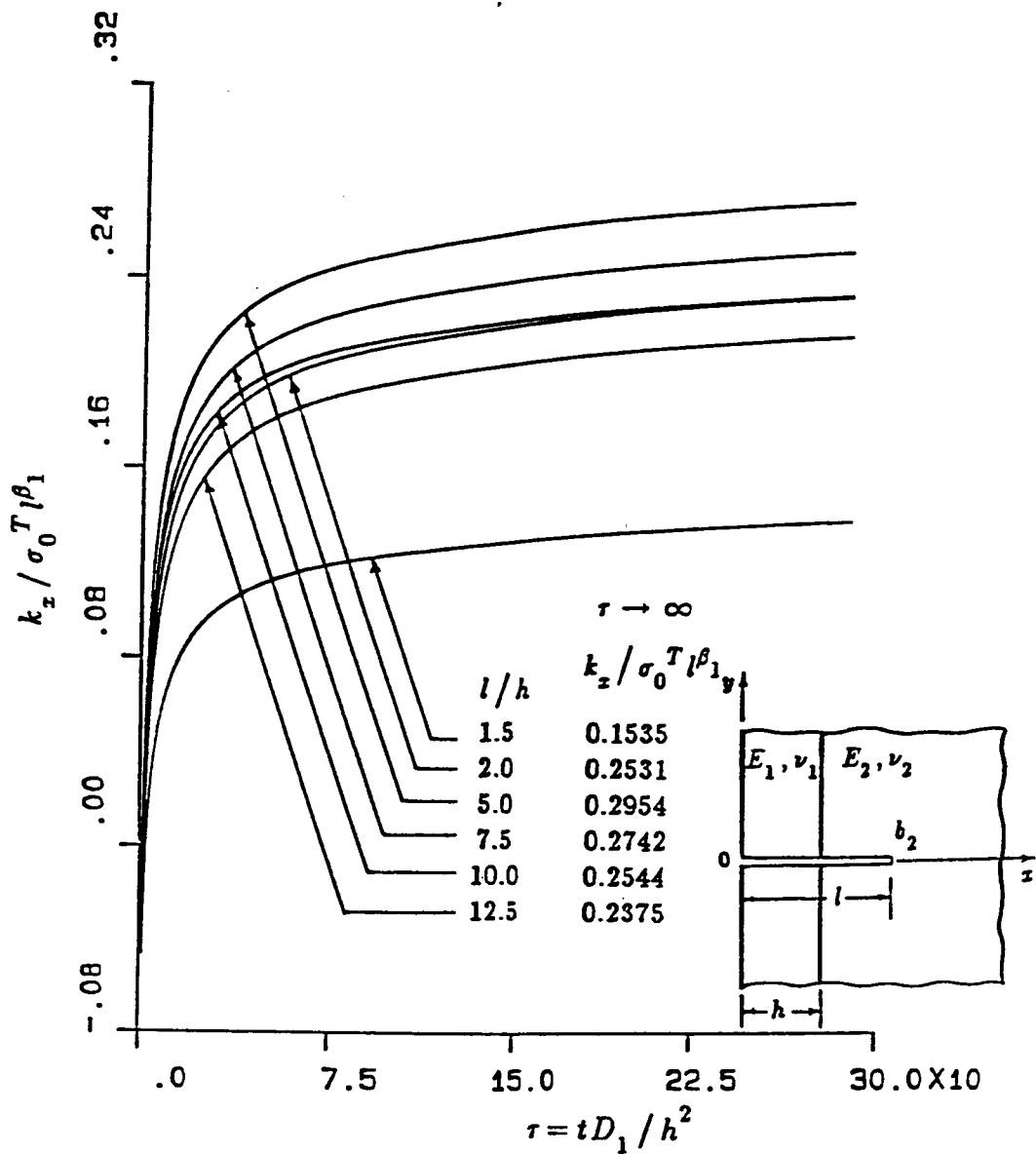b_1=ħ=a_2)

Fig. 24 The normalized stress intensity factor $k_{xx}/\sigma_0 \ell^\beta$ in material pair B with an edge crack crossing the interface; ($\tau_0=0$, $\ell=b_2$, $a_1=0$, $b_1=h=a_2$, $\sigma_{ij} \sim r^{-\gamma}$, $\beta=0.01872238$)
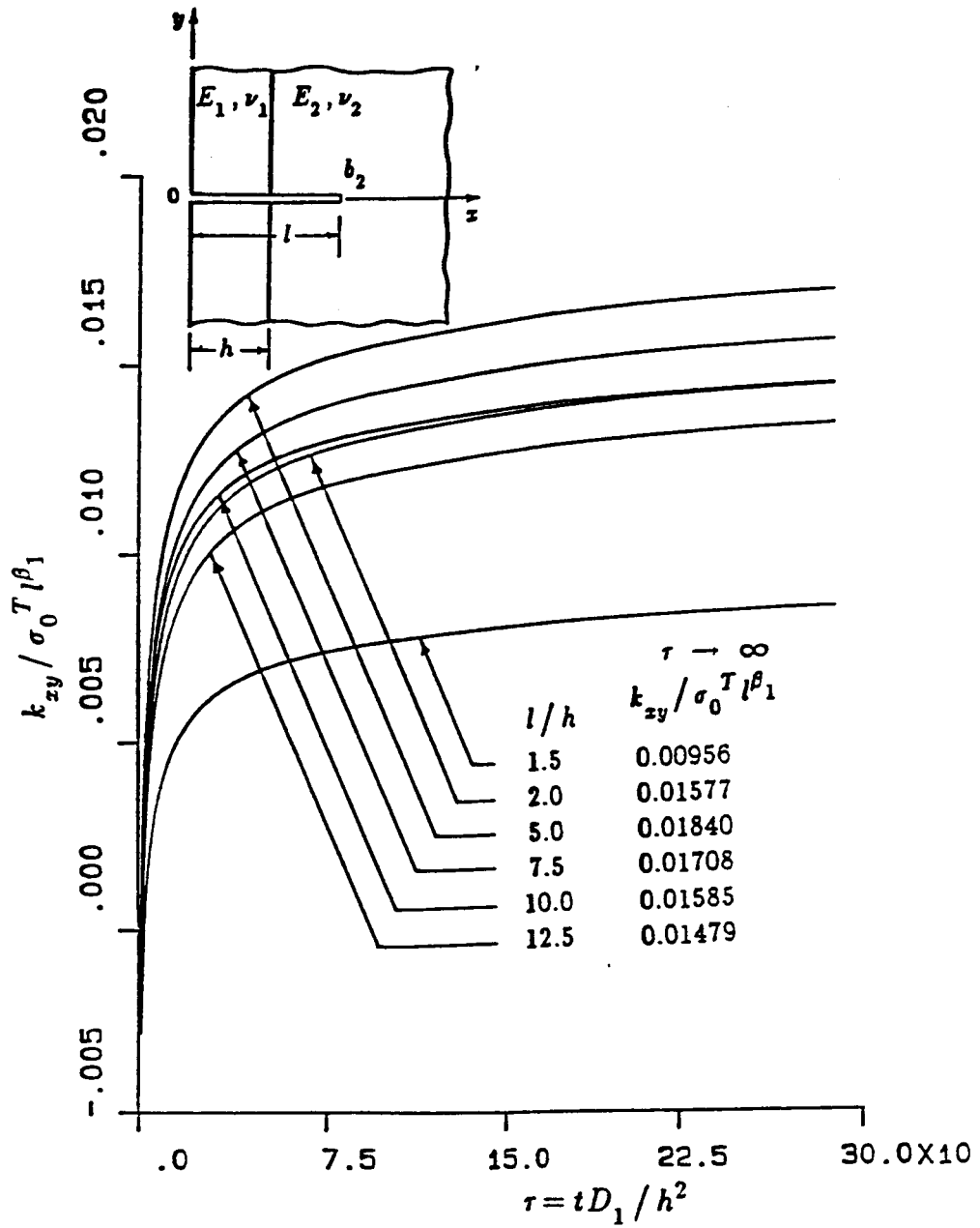
Fig. 25   The normalized stress intensity factor $k_{xy}/\sigma_0 \ell^\beta$ in material pair B with an edge crack crossing the interface; ($\tau_0 = 0$, $\ell = b_2$, $a_1 = 0$, $b_1 = h = a_2$, $\beta = 0.01872238$)